Extracellular TGF-β downregulates the expression of Wnt transcription factor TCF7L2/TCF4 in mesenchymal stromal cells and fibroblasts

Osvaldo Contreras[1,2,*], Hesham Soliman[2,3], Marine Theret[2], Fabio M. Rossi[2], Enrique Brandan[1,*]

[1]Departamento de Biología Celular y Molecular and Center for Aging and Regeneration (CARE-ChileUC), Facultad de Ciencias Biológicas, Pontificia Universidad Católica de Chile, 8331150 Santiago, Chile. [2]Biomedical Research Centre, Department of Medical Genetics and School of Biomedical Engineering, University of British Columbia, V6T 1Z3 Vancouver, BC, Canada. [3]Faculty of Pharmacy, Minia University, 61519 Minia, Egypt

*Authors for correspondence (oicontre@uc.cl; ebrandan@bio.puc.cl)

Authors' e-mails:
Osvaldo Contreras: oicontre@uc.cl
Hesham Soliman: hesham@brc.ubc.ca
Marine Theret: mtheret@brc.ubc.ca
Fabio M. Rossi: fabio@brc.ubc.ca
Enrique Brandan: ebrandan@bio.puc.cl

Keywords: Wnt signaling, Stem cells, Regeneration, Fibrosis, Fibroblasts, Myoblasts

Summary statement

TGF-β signaling suppresses the expression of the Wnt transcription factor TCF7L2 and compromises TCF7L2-dependent function in fibroblasts.

Abbreviations

Cycloheximide, CHX

Connective tissue, CT

Duchenne muscular dystrophy, DMD

Extracellular matrix, ECM

Fibro-adipogenic progenitors, FAPs

Fluorescence-activated cell sorting, FACS

Histone deacetylases, HDACs

Mesenchymal stromal cells, MSCs

Muscle stem cells, MuSCs

Muscular dystrophy, MD

Platelet-derived growth factor receptor alpha, PDGFRα

T-cell factor/lymphoid enhancer, Tcf/Lef

Transcription factor, TF

Transforming growth factor type-beta, TGF-β

Trichostatin A, TSA

Tumor necrosis factor alpha, TNF-α

Ubiquitin-proteasome system, UPS

ABSTRACT

Mesenchymal stromal cells (MSCs) are multipotent progenitors essential for organogenesis, tissue homeostasis, regeneration, and scar formation. Tissue injury upregulates TGF-β signaling, which plays predominant roles in MSCs fate, extracellular matrix (ECM) remodeling, and fibrogenesis. However, the molecular determinants of MSCs differentiation and survival are still poorly understood. The canonical Wnt Tcf/Lef transcription factors are important players in development and stem cell fate, but the mechanisms by which injury-induced signaling cues regulate the expression of Wnt Tcf/Lef remain poorly understood. Here, we studied the cell-specific gene expression of Tcf/Lef in MSCs and, more specifically, investigated whether damage-induced TGF-β affects the expression and function of TCF7L2 using different *in vitro* models of MSCs, including fibro-adipogenic progenitors. We demonstrated that Tcf/Lef members are differentially expressed in MSCs and that TGF-β signaling impairs TCF7L2 expression in these cells but not in myoblasts. Also, we show that the ubiquitin-proteasome system (UPS) regulates TCF7L2 proteostasis and participates in TGF-β-mediated TCF7L2 protein downregulation. Finally, we also show that TGF-β requires HDACs activity to repress the expression of TCF7L2 in fibroblasts. Thus, our work establishes a novel molecular interplay between TGF-β and Wnt signaling cascades in stromal cells and suggests that this mechanism could be targeted in tissue fibrosis.

INTRODUCTION

The remarkable long-term capacity to grow and regenerate of adult skeletal muscle is largely based on the presence of tissue-resident muscle stem cells (MuSCs) (formerly named as satellite cells) (Lepper et al., 2011; Murphy et al., 2011; Sambasivan et al., 2011). However, another tissue-resident population of mesenchymal stromal cells (MSCs) is also an essential component for effective regeneration and maintenance of skeletal muscle and its connective tissue (CT). MSCs regulate extracellular matrix (ECM) modeling and remodeling, MuSCs biology, muscle regeneration and maintenance (Heredia et al., 2013; Joe et al., 2010; Mathew et al., 2011; Uezumi et al., 2010; Wosczyna et al., 2019). These stromal cells are also called fibro-adipogenic progenitors (FAPs) in mouse and human skeletal muscle (Agley et al., 2013; Dulauroy et al., 2012; Uezumi et al., 2014a; Vallecillo-García et al., 2017; Wosczyna and Rando, 2018). MSCs have the potential to differentiate *in vivo* and *in vitro* into myofibroblasts, adipocytes, chondrogenic, and osteogenic cells (Agley et al., 2013; Contreras et al., 2019c; Oishi et al., 2013; Uezumi et al., 2014b; Uezumi et al., 2011; Wosczyna et al., 2012). These PDGFRα^+ MSCs are found in most tissues, including bone marrow, heart, kidney, muscle, nerves, liver, lung, and skin in which they play crucial roles (Carr et al., 2019; Lemos and Duffield, 2018; Lynch and Watt, 2018; Rognoni et al., 2018). Despite their required normal activity during muscle regeneration (Joe et al., 2010; Heredia et al., 2013; Mathew et al., 2011; Fiore et al., 2016; Wosczyna et al., 2019), we and others have reported dysregulated behavior of these precursor cells in models of acute and chronic muscle damage, muscular dystrophy (MD), neurodegenerative diseases, and aging (Acuña et al., 2014; Contreras et al., 2016; Contreras et al., 2019c; González et al., 2017; Kopinke et al., 2017; Madaro et al., 2018; Mahmoudi et al., 2019; Lemos et al., 2015; Lukjanenko et al., 2019; Uezumi et al., 2014a). A common outcome of the dysregulation of these cells is fibrosing disorders, which include non-malignant fibroproliferative diseases with high morbidity and mortality (Lemos and Duffield, 2018; Wynn and Ramalingam, 2012). Therefore, a better knowledge of MSCs biology and the molecular and cellular mechanisms that govern their activity might contribute to accelerating the development of much overdue therapeutics for the treatment of several scar-forming pathologies.

Wnt signaling pathway has a key role in many aspects of developmental biology, tissue homeostasis, stem cells fate, organogenesis, disease (especially cancer), and tissue fibrogenesis. Secreted Wnt ligands, which are 19 secreted lipid-modified

glycoproteins, bind to the Frizzled receptors and its co-receptor LRP5/6 on the cell surface to initiate a signaling pathway that regulates the proteostasis of cytoplasmic β-catenin. In the absence of canonical Wnt ligands, β-catenin is a target for the ubiquitin–proteasome pathway-mediated degradation (Aberle et al., 1997). Once the canonical cascade starts, the accumulation of β-catenin leads to its translocation to the nucleus, where it recognizes and binds the T-cell factor (TCF) or Lymphoid enhancer (LEF) transcription factors (TFs) but also recruits transcriptional partners and chromatin remodeling complexes which in concert regulate the expression of Tcf/Lef target genes. Tcf/Lef TFs recognize Tcf/Lef-binding elements on its target genes to regulate the expression of thousands of genes (Cadigan and Waterman, 2012; Clevers, 2006; Schuijers et al., 2014). Therefore, the Tcf/Lef transcription factors (TFs) are the final effectors of the canonical Wnt/β-catenin signaling cascade in metazoans (Nusse and Clevers, 2017; Schuijers et al., 2014; Tang et al., 2008). Mammalian cells express four Tcf/Lef protein-coding genes: Tcf1 (Tcf7), Lef1, Tcf7l1 (formerly named Tcf3), and Tcf7l2 (formerly named Tcf4) (Cadigan and Waterman, 2012; van de Wetering et al., 1991). They have critical roles regulating the body plan establishment, cell fate specification, proliferation, survival, and differentiation, which are predominant features in fast and constantly renewing tissues (Clevers, 2006; Korinek et al., 1998). Accumulating evidence indicates that pathologically activated canonical Wnt signaling plays a major role in the pathogenesis of fibrosis in multiple tissues, including skin, liver, lung, kidney and the heart (Chilosi et al., 2003; Colwell et al., 2006; Cosin-Roger et al., 2019; He et al., 2009; He et al., 2010; Henderson et al., 2010; Konigsho et al., 2008; Liu et al., 2009; Surendran et al., 2002; Trensz et al., 2010; Wei et al., 2011). Furthermore, upregulated Wnt activity during aging accounts in part for the declining regenerative potential of muscle with age and increased fibrosis (Brack et al., 2007). For example, the conditional genetic loss of β-catenin in cardiac fibroblasts lineages ($Tcf21^{+}$ or $Periostin^{+}$) causes the reduction of interstitial fibrosis and attenuates heart hypertrophy induced by cardiac pressure overload (Xiang et al., 2017). Mechanistically, it has been demonstrated that Wnt/β-catenin pathway regulates the expression of several ECM genes in fibroblasts from different organs (Akhmetshina et al., 2012; Hamburg-Shields et al., 2015; Xiang et al., 2017). Altogether, these studies suggest that Wnt/β-catenin signaling in stromal cells is required for pathogenic extracellular matrix gene expression and collagen deposition during fibrogenesis.

Transforming growth factor type-beta (TGF-β) regulates the differentiation program of a variety of cell types (for review see David and Massagué, 2018; Derynck and Budi, 2019), including MSCs. TGF-β regulates MSCs and/or fibroblast activation via enhancing their proliferation and by up-regulating ECM genes in fibrotic diseases (Ceco and McNally, 2013; Smith and Barton, 2018; Wynn and Ramalingam, 2012). Three TGF-β isoforms - TGF-β1, TGF-β2, and TGF-β3- are expressed in mammals (Massagué, 1998). These isoforms and their mediated signaling pathways are exacerbated in Duchenne muscular dystrophy (DMD) patients (Bernasconi et al., 1999; Smith and Barton, 2018) and skeletal muscles of the *mdx* mice (Acuña et al., 2014; Gosselin et al., 2004; Lemos et al., 2015), and during fibrogenesis in several organs (Kim et al., 2018). Thus, it is recognized that dysregulated TGF-β activity is a driver for reduced muscle regeneration, impaired tissue function and fibrosis (Mann et al., 2011; Pessina et al., 2015; Vidal et al., 2008). Interestingly, TGF-β inhibition improves the pathophysiology of MD (Accornero et al., 2014; Acuña et al., 2014; Ceco and McNally, 2013; Cohn et al., 2007; Danna et al., 2014). Mechanistically, TGF-β signaling stimulates FAPs and MSCs proliferation, extracellular matrix (ECM) production and myofibroblast differentiation (Contreras et al., 2019b; Hinz et al., 2007; Lemos et al., 2015; Uezumi et al., 2011). Hence, understanding the role of TGF-β signaling in MSCs may offer novel opportunities for the development of effective anti-fibrotic strategies and to improve tissue function.

Growing evidence suggests that the Wnt signaling pathway, previously recognized by its essential role in development, also has crucial functions in regeneration and repair (reviewed in Burgy and Königshoff, 2018; Cisternas et al., 2014; Degirmenci et al., 2018; Girardi and Le Grand, 2018; Nusse and Clevers, 2017; Oliva et al., 2018; Tan and Barker, 2018). During the last decade, emerging studies suggest a functional crosstalk between Wnt cascade and TGF-β signaling in modulating MSCs activation and fate (Biressi et al., 2014; Burgy and Königshoff, 2018; Cosin-Roger et al., 2019; Vallée et al., 2017; Hamburg-Shields, et al., 2015). For example, the canonical Wnt3a ligand upregulates TGF-β signaling via Smad2 in a β-catenin-dependent mechanism, and therefore, promotes the differentiation of fibroblasts into myofibroblasts (Carthy et al., 2011). Transgenic mice overexpressing canonical Wnt-10b demonstrated that activation of this pathway is sufficient to induce fibrosis *in vivo* (Akhmetshina et al., 2012). TGF-β promotes the secretion of Wnt proteins, via transforming growth factor beta-activated kinase 1 activation, which in turn activates the canonical Wnt cascade (Blyszczuk et al., 2016). Therefore, this

TGF-β-dependent Wnt secretion induces myofibroblasts formation and myocardial fibrosis progression (Blyszczuk et al., 2016). Elevated canonical Wnt signaling is found in dystrophic *mdx* muscles and controls MuSCs fate via cross-talk with TGF-β2 signaling (Biressi et al., 2014). Also, a recent study demonstrated that TGF-β induces the production of the canonical ligand Wnt3a, which in turn increases TGF-β secretion, establishing an amplification circuit between TGF-β and Wnt signaling pathways in cardiac fibroblasts (Seo et al., 2019). Therefore, these studies demonstrate novel cross-talk between TGF-β and the canonical Wnt pathway. Whether TCF7L2 expression and function could be modulated by TGF-β is of interest to increase our incipient understanding in CT biology, MSCs fate, and lately their participation in the development of fibrosis as a predominant cell source of ECM.

In the present study, first, we investigated the cell-specific expression of the four Tcf/Lef family members in several MSC *in vitro* and *ex vivo* models. Second, we studied the effect of TGF-β signaling on Tcf7l2 expression and function in stromal cells. By combining *in vitro* and *in silico* analyses we demonstrate; first, that Tcf7l2 is a novel valid TGF-β-downregulated target gene in MSCs and fibroblasts, and second, that the ubiquitin-proteasome system (UPS) participates, both, in TCF7L2 proteostasis and TGF-β-mediated TCF7L2 protein downregulation. Finally, the effects of TGF-β signaling on the expression of TCF7L2 were not observed in myogenic cells, suggesting that this crosstalk is fibroblast/MSC specific.

RESULTS

Wnt Tcf/Lef transcription factors are differentially expressed in mesenchymal stromal cells and fibroblasts

We first determined the relative expression of the Wnt T-cell factor/Lef members in the mesenchymal stromal/stem cell line C3H/10T1/2 and mouse embryonic fibroblasts (MEFs) (Fig. 1A). *Tcf7l1* and *Tcf7l2* were the two most highly expressed members of this family, while *Lef1* and *Tcf7* were almost not expressed by MSCs or MEFs (Fig. 1A). Then, we evaluated the expression of these transcription factors in *ex vivo* FACS-isolated skeletal muscle PDGFRα-H2BEGFP^{+} FAPs (Fig. 1B, Fig. S1A). Our results using *ex vivo* stromal cells further corroborated the observations described above (Fig. 1C). Thus, these results suggest that among the Wnt Tcf/Lef members, *Tcf7l1* and *Tcf7l2* but not *Lef1* or *Tcf7*, were highly expressed in MSCs and fibroblasts. We next evaluated TCF7L2 protein expression in skeletal muscle tissue and MSCs. The protein products detected by western blotting in most tissues and cells are ~78 and ~58 kDa in size (Jin, 2016; Tang et al., 2008; Weise et al., 2010). We found that these TCF7L2 protein isoforms are present in limb muscles and MSCs, representing the E and M/S isoforms (Fig. 1D, Fig. S1B) (Contreras et al., 2016; Jin, 2016; Weise et al., 2010). We also found that the TCF7L2 TF is predominantly expressed in the nucleus of tissue-resident interstitial cells in the undamaged diaphragm muscle, isolated EGFP^{+} FAPs from the PDGFRα^{H2BEGFP}, *mdx*;PDGFRα^{H2BEGFP} dystrophic mice, and MEFs (Fig. 1E, Fig. S1B-D). The tissue-specific expression of the Tcf/Lef members and their relative expression in MSCs was further corroborated by additional data obtained from the Murine Tabula Muris database (Fig. S1F,G) (The Tabula Muris Consortium et al., 2018). Next, we evaluated the expression of TCF7L2 protein in transiently-activated adult FAPs (Fig. 1F) and confirmed that it is present three days after notexin injury (Fig. 1G). Stromal fibroblasts are also found in the heart playing supportive roles in cardiac development and repair (Farbehi et al., 2019; Fu et al., 2018; Furtado et al., 2016; Soliman et al., 2019 preprint; Tallquist and Molkentin, 2017). Hence, we evaluated the relative expression of the Tcf/Lef family members in heart fibroblasts. Similar to what we found for skeletal muscle FAPs, *Tcf7l1* and *Tcf7l2* are the two most highly expressed members of this family in cardiac fibroblasts whereas *Lef1* and *Tcf7* members have very low expression levels (Fig. 1H). Similar to muscle, both E and M/S TCF7L2 protein isoforms were also found in cardiac tissue (Fig. 1I,J). Altogether, these results establish that specific Tcf/Lef transcription factors, namely TCF7L2, are

highly expressed in MSCs and fibroblasts as well as total skeletal muscle and cardiac tissue.

Dynamics of TCF7L2 expression in stromal fibroblasts during regeneration and repair

Others and we have demonstrated that sub-populations of stromal MSCs co-express both TCF7L2 and the tyrosine kinase receptor PDGFRα in development and adulthood (Contreras et al., 2016; Contreras et al., 2019a,b; Murphy et al., 2011; Vallecillo-García et al., 2017). As a consequence of the stromal expansion caused by injury both TCF7L2 and PDGFRα protein levels are increased in dystrophic tissue, denervated muscle, and after chronic barium chloride-induced damage (Contreras et al., 2016). Interestingly, the number of TCF7L2$^+$ cells in skeletal muscles of the *mdx* mice correlated with the extension of damage, fibrosis, and TGF-β levels (Contreras et al., 2016). Thus, more TCF7L2$^+$ MSCs are detected in the diaphragm than in the gastrocnemius, with fewer cells in the tibialis anterior, when compared to wild type muscles (Contreras et al., 2016). The described correlation between the degree of damage and TCF7L2 total protein levels was also seen in muscular dystrophy (Contreras et al., 2016; Contreras et al., 2019a). Additionally, TCF7L2$^+$ MSCs expansion in human regenerating muscle closely associates with regenerating myofibers *in vivo* (Mackey et al., 2017). Thus, to study whether the expression of TCF7L2 changes during regeneration and repair, we used two common muscle injury models previously described (Uezumi et al., 2010; Kopinke et al., 2017). First, we aimed to study whole tissue TCF7L2 protein levels during regeneration following glycerol-induced acute skeletal muscle damage, a model that leads to transient stromal expansion (Contreras et al., 2019c; Kopinke et al., 2017). As expected, glycerol acute damage caused an increase of total TCF7L2 protein levels, which transiently peak at day 3 following glycerol intramuscular injection (Fig. 2A,B). PDGFRα protein levels varied with similar kinetics of expression as TCF7L2 after acute injury (Fig. 2A,B). We also found that the transcriptional partner of TCF7L2, β-Catenin, increased after acute damage (Fig. 1A,B). Myosin heavy chain expression peaked at day 7 of damage (Fig. 2A,B). As mentioned above, we previously described that TCF7L2$^+$ stromal cells and the whole tissue expression of TCF7L2 increases in the dystrophic diaphragm (Fig. 2C,D) (Contreras et al., 2016). Intriguingly, we found a reduction in the expression levels of TCF7L2 in the expanded population of TCF7L2$^+$ cells in the dystrophic diaphragm, where the proportion of TCF7L2$^+$ cells expressing low levels of TCF7L2 was larger compared to undamaged

muscle. In the latter case, TCF7L2 expression was generally high (Fig. 2C). To further explore our initial observation in Fig. 2C, we used confocal microscopy and z-stack reconstructions of transverse muscle sections to analyze the cellular amount of TCF7L2 in stromal cells in the dystrophic diaphragm (Fig. 2C,E, Fig S1H). TCF7L2^{high} cells were distributed throughout the muscle interstitium as defined using laminin-α2, consistent with previous studies of stromal distribution (Fig. 2c, Fig. S2H) (Contreras et al., 2016; Contreras et al., 2019c; Mathew et al., 2011; Merrell et al., 2015; Murphy et al., 2011). On the other hand, TCF7L2$^{medium/low}$-expressing cells accumulated and their expansion corresponded to increased phosphorylation of Smad3 -an index of activated TGF-β signaling- in interstitial cells and muscle fibers, as well as in collagen type 1-enriched areas (Fig. 2E-H, Fig. S2H). These results suggest that the magnitude of expansion of TCF7L2$^{medium/low}$ cells depends on the extent of tissue inflammation, TGF-β levels, damage, and fibrosis, and hence they were abundant in the inflammatory dystrophic model.

TGF-β signaling downregulates the expression of the WNT TCF7L2 transcription factor in FAPs, MSCs and fibroblasts

Chronic upregulation of TGF-β is found in several models of organ damage, where it is known to regulate tissue fibrosis severity (Kim et al., 2018; Pessina et al., 2015). Activated extracellular TGF-β not only promotes MSCs survival and proliferation but also primes these progenitor cells to become myofibroblasts (Contreras et al., 2019b, Contreras et al., 2019c; Cho et al., 2018; Kim et al., 2018; Lemos et al., 2015). TCF7L2^{+} MSCs are closely associated with CD68^{+} macrophages (one of the major cell sources of TGF-β in DMD) (Bentzinger et al., 2013; Contreras et al., 2016; Juban et al., 2018; Tidball and Villalta, 2010). Our previous results suggest that damage and inflammation negatively correlate with TCF7L2 expression in MSCs. Hence, damage-associated signaling pathways might regulate TCF7L2 expression and function endogenously during tissue repair. Therefore, we aimed to investigate the role of TGF-β signaling on the expression of TCF7L2 in fibroblast-related cell types and tissue-resident stromal cells. We first used the multipotent mesenchymal progenitor cell line C3H/10T1/2 as an *in vitro* model of MSCs, because these cells have been extensively used to study mesenchymal biology (Braun et al., 1989; Contreras et al., 2019c; Reznikoff et al., 1973; Riquelme-Guzman, et al., 2018; Singh et al., 2003). TGF-β1 diminished TCF7L2 protein expression in C3H/10T1/2 MSCs in a concentration-dependent manner, with effects already noticeable at the physiologically relevant concentration of 0.5 ng/ml (Fig. 3A,B, Fig. S2A,B). We confirmed that C3H/10T1/2

cells respond to TGF-β1, in a concentration dependent-manner, by increasing the expression of ECM-related proteins (fibronectin, β1-Integrin, CCN2/CTGF) and αSMA (myofibroblasts marker), as well as reducing PDGFRα expression (Fig. 3A,B) (Contreras et al., 2019c). Moreover, TGF-β1-mediated reduction of TCF7L2 expression began at 8 h after stimulation, reaching a maximum at 24 and 48 h at which point the expression of TCF7L2 was diminished by 75-80 per cent (Fig. 3C,D). Similar effects were also seen in the embryonic fibroblast NIH-3T3 cell line (Fig. 3E,F, Fig. S2A). Taken together, these results suggest that TGF-β downregulates TCF7L2 protein expression in a concentration- and time-dependent manner in MSCs and fibroblasts. Then, we used *ex vivo* FAPs isolated from undamaged limb muscles. Consistently with the above-mentioned results, we found that TGF-β1 reduced the expression of TCF7L2 by ~50% in FAPs (Fig. 3G,H). As expected, TGF-β increased the expression of the ECM protein fibronectin (Fig. 3G) (Uezumi et al., 2010; Contreras et al., 2019c). Taken together, our results indicate that, along with inducing fibroblasts activation, TGF-β also inhibits the expression of Tcf7l2 in skeletal muscle FAPs, and in two different mesenchymal cell lines, C3H/10T1/2 and NIH-3T3 fibroblasts.

Not only the TCF7L2 protein levels were decreased in response to TGF-β, but also the relative levels of *Tcf7l2* mRNA diminished 2 h, 8 h and 24 h after TGF-β1 stimulation (Fig. 3I). *Tcf7l2* gene expression was also sensitive to the inhibition of mRNA synthesis with actinomycin D treatment, which suggests active *Tcf7l2* gene transcription and TCF7L2 translation in MSCs (Fig. 3J, Fig. S2C-E). The expression of PDGFRα was also very sensitive to the inhibition of mRNA synthesis with actinomycin D in MSCs (Fig. 3J, Fig. S2C). In addition to TGF-β1, TGF-β2 and TGF-β3 are also mammalian extracellular TGF-β isoforms with biological activity in fibroblasts (David and Massagué, 2018; Derynck and Budi, 2019; Kim et al., 2018). Hence, we evaluated whether these cytokines impair TCF7L2 expression in MSCs. Similar to TGF-β1, both TGF-β2 and TGF-β3 strongly reduced TCF7L2 protein levels in MSCs (Fig. S2F,G). Thus, the three TGF-β cytokines decrease TCF7L2 expression in mesenchymal stromal cells. Next, to investigate whether the function of the Wnt-effector TCF7L2 was also altered by TGF-β, we determined, by quantitative PCR, the gene expression level of several validated TCF7L2 target genes in response to TGF-β. The expression of *Sox9*, *Axin2*, and *Tcf7l1* was repressed, while *Nfatc1*, *Lef1*, and *Tcf7* expression was increased in response to TGF-β1 (Fig. S2H). We

did not find changes in *β-Catenin* or *Ccnd1* mRNA levels (Fig. S2H). Altogether, these data suggest that TGF-β signaling reduces the expression of TCF7L2, and therefore, alters its TF function in mesenchymal stromal cells, such as FAPs, MSCs, and fibroblasts. Since TGF-β-induced myofibroblast differentiation of MPCs correlates with reduced TCF7L2 expression and impaired function, we investigated the impact that differentiation *in vitro* towards other lineages such as adipocytes and osteocytes might have on Tcf7l2 gene expression. We used the expression of *Adipoq* and *Runx2* as markers of effective adipogenic and osteogenic commitment of MEFs (Fig. S3). Adipogenic differentiation did not alter *Tcf7l2* mRNA expression (Chen et al., 2018), while increased *Tcf7l2* mRNA levels were found after osteogenic differentiation (Fig. S3). Interestingly, the gene expression of *Tcf7l1*, *Lef1* and *Tcf7* also varied in response to adipogenic or osteogenic differentiation (Fig. S3). These data suggest that different molecular mechanisms are involved in the regulation of *Tcf7l2* gene expression during differentiation to different cell lineages.

Extracellular TGF-β reduces the expression of TCF7L2 in a TGF-β receptor type-I-dependent manner

Having detected a drop in the total levels of TCF7L2 TF, we next determined the extent of TCF7L2 protein decrease in the nuclei of TGF-β-treated cells. A subcellular fractionation method (see Materials and Methods section for details) allowed us to determine that TCF7L2 TF was relatively abundant in the nucleus, although TCF7L2 protein was also detected in MSC cytoplasm (Fig. S4A,B). TGF-β stimulation downregulated the expression of TCF7L2 in both the nuclear and cytoplasmic fractions (Fig. 4A, Fig. S4A,B). Next, we further studied the association between TGF-β-mediated fibroblast activation and reduced TCF7L2 levels at the cellular level. Using confocal microscopy, we observed that TCF7L2 nuclear expression was diminished in response to TGF-β and that TCF7L2 repression correlated with TGF-β-induced myofibroblast phenotype in FAPs and NIH-3T3 fibroblasts (Fig. 4B,C, Fig. S4C). In addition, TGF-β signaling did not alter TCF7L2 protein subcellular distribution or nuclei-cytoplasm shuttle (Fig. 4D,E). Overall, these data indicate that TGF-β, in addition to inducing the differentiation of MSCs and fibroblasts into myofibroblasts, also represses the expression of the Wnt-effector TCF7L2. Then, to investigate the role of TGF-β receptors in the regulation of TCF7L2 by TGF-β, we used the TGFBR1 specific small-molecule inhibitor SB525334 (Callahan et al., 2002). TGF-βs ligand binding to the type II receptor TGFBR2 leads to recruitment and phosphorylation of the type I receptor

ALK-5 (TGFBR1). The treatment with the TGFBR1 inhibitor completely abolished the downregulation of TCF7L2 expression by TGF-β1 in wild-type FAPs and C3H/10T1/2 MSCs without affecting the total levels of the TCF7L2-binding partner β-catenin (Fig. 4F,G). These data suggest that TGF-β-mediated TCF7L2 downregulation requires the activation of TGF-β receptors signaling cascade.

TGF-β requires HDACs to repress TCF7L2 gene expression

The TGF-β family acts via Smad and non-Smad signaling pathways to regulate several cellular responses (Derynck and Budi, 2019; Zhang, 2017). To investigate the role of Smad and non-Smad cascades in the regulation of TCF7L2 by TGF-β, we used specific small-molecule inhibitors of Smad3, p38 MAPK, JNK, and ERK1/2 (Fig. 5A). None of these inhibitors were able to abolish the effect of TGF-β1 on the expression of TCF7L2 (Fig. 5A,B). Although we recently found that p38 MAPK participates in TGF-β-mediated downregulation of PDGFRα expression (Contreras et al., 2019c), we did not detect any significant effect of the p38 MAPK inhibitor SB203580 co-treatment on TGF-β-induced TCF7L2 downregulation (Fig. 5A,B, Fig. S5A). Interestingly, we found that SIS3 (a Smad3 inhibitor) co-treatment augmented the inhibitory effect of TGF-β on the expression of TCF7L2 (Fig. 5A,B, Fig. S5B). Overall, these results suggest that another, not yet identified Smad-independent pathway may participate in TGF-β-mediated downregulation of TCF7L2 expression.

It has been suggested that TCF7L2 might be a non-histone target of histone deacetylases (HDACs). This was based on the observation that treatment with trichostatin A (TSA), a commonly used histone deacetylase inhibitor (HDI), reduced the protein expression of TCF7L2 in the human colon cancer cell type HCT116 cells by 50% (Götze et al., 2014). Since HDAC regulate transcription of many genes (Bolden et al., 2006; Greet et al., 2015; Seto and Yoshida, 2014), we first evaluated whether TSA affects TCF7L2 protein levels in MSCs. Indeed, TSA treatment reduced TCF7L2 levels, although to a lesser extent when compared to TGF-β (Fig. 5C,D). Based on recent findings that demonstrated that TGFβ-mediated fibroblast activation requires HDAC-mediated transcriptional repression (Jones et al., 2019), we examined whether inhibiting HDACs with TSA may modify TGF-β-mediated reduction of TCF7L2 expression. we examined whether inhibiting HDACs with TSA may alter TCF7L2 expression in response to TGF-β signaling. Therefore, the cells were treated with TGF-β1 and/or TSA for 8 h and TCF7L2

protein levels were then evaluated by western blot. Interestingly, whereas TGF-β1 decreased TCF7L2 expression, TSA partially blocked TGF-β-mediated repression of TCF7L2 expression (Fig. 5E,F). RNA sequencing analysis from recent work on lung fibroblasts helped us to corroborate our results (Fig. 5G) (Jones et al., 2019). The pan HDAC inhibitor, pracinostat, attenuates TGF-β-induced repression of Tcf7l2 gene expression (Fig. 5G). Taken together, these data suggest that HDACs participate in TGF-β-mediated regulation of TCF7L2 expression levels.

TGF-β reduces TCF7L2 protein levels by stimulating protein degradation via the ubiquitin-proteasome system

To gain knowledge of the mechanisms involved in TGF-β-induced TCF7L2 repression, we performed a time-course analysis with the protein synthesis inhibitor cycloheximide. Thus, we determined that TCF7L2 protein half-life is quite short, being approximately 3.5 h in both proliferating C3H/10T1/2 MSCs and FAPs ($T_{1/2}$=3.5 h) (Fig. 6A-C). Then, to study the molecular mechanism governing TGF-β-mediated TCF7L2 downregulation we evaluated the human TCF7L2 interactome using BioGRID datasets (Stark et al., 2006). Interestingly, several protein-quality-control-related proteins were interacting partners of TCF7L2, among them: RNF4, RNF43, RNF138, NLK, UHRF2, UBE2I, UBE2L6, USP4, UBR5, and XIAP (Fig. 6D). Since these TCF7L2 interacting proteins belong to or are related to the ubiquitin-proteasome system (UPS), we performed *in silico* analyses and identified several top-ranked potential ubiquitination sites along the TCF7L2 protein sequence (Fig. 6E). Next, we used MG132, a potent proteasome inhibitor that reduces the degradation of ubiquitin-conjugated proteins (Nalepa et al., 2006), to evaluate the participation of the UPS in the downregulation of TCFL72 by TGF-β. Mechanistically, MG132 completely blocked TGF-β-mediated downregulation of TCF7L2 protein after 9 h of co-treatment in MSCs and FAPs (Fig. 6F,G, Fig. S6A,B). MG132 also increased TCF7L2 basal protein levels when used alone, which suggests that an intrinsic ubiquitin-mediated protein degradation mechanism controls the TCF7L2 steady-state levels (Fig. 6F,G, Fig. S6). Remarkably, a more resolving SDS-PAGE gel (12%) allowed us to identify an unknown higher molecular weight form (~65-70 kDa) of TCF7L2 not present at steady-state, but sensitive to proteasome-mediated proteolysis inhibition by MG132 (Fig. S6B). Finally, because our BioGRID analysis suggests the interaction of TCF7L2 with deubiquitinating enzymes -that remove conjugated ubiquitin from target proteins- we evaluated the amount of TCF7L2

protein in C3H/10T1/2 MSCs treated with the ubiquitin-specific protease 7 (USP7) small-molecule inhibitor HBX 41108 (HBX) in proliferating conditions (Colland et al., 2009; Yuan et al., 2018). The treatment with HBX diminished TCF7L2 protein levels in a time-dependent manner (Fig. 6H). We also found that HBX-mediated TCF7L2 degradation was sensitive to the inhibition of protein synthesis (Fig. 6H). Taken together, these results suggest the participation of the ubiquitin-proteasome system in the regulation of TCF7L2 steady-state proteostasis and TGF-β-mediated repression of TCF7L2 protein expression.

TCF7L2 expression and subcellular localization is not affected by TGF-β in C2C12 myoblasts

Myoblasts are known to respond to TGF-β signaling (Droguett et al., 2006; Massagué et al., 1986; Riquelme et al., 2001; Schabort et al., 2009). For example, TGF-β1 induces a pro-fibrotic-like phenotype of myoblasts by inducing the expression of ECM-related proteins (Riquelme-Guzman et al., 2018). Therefore, we investigated whether TCF7L2 downregulation by TGF-β signaling was stromal cell-type-specific or whether it also occurred in myoblasts. C2C12 myoblasts express very low levels of TCF7L2 transcription factor and β-catenin when compared to C3H/10T1/2 MSCs (Fig. 7A,B, Fig. S7A,B). Similar to what we found in stromal cells, TCF7L2 protein was expressed predominantly in myoblasts' nuclei (Fig. S7A). However, TGF-β1 stimulation did not alter the expression of TCF7L2, both at the protein and mRNA levels, in C2C12 myoblasts at the different concentrations used for 24 or 48 h (Fig. 7C-E, Fig. S7C,D). However, myoblasts did respond to TGF-β by increasing the expression of the two ECM components fibronectin and the matricellular protein CCN2/CTGF (Fig. 7C,E, Fig. S7C), as previously reported (Riquelme-Guzmán et al., 2018; Vial et al., 2008). Finally, we did not find changes in TCF7L2 subcellular distribution in myoblasts after TGF-β treatment (Fig. 7F,G, Fig. S7E). Thus, although TGF-β induces myoblasts activation it does not change the expression of the TCF7L2 transcription factor, which is relatively low in these cells when compared to stromal cells and fibroblasts. Overall, these results suggest that TGF-β-mediated mechanisms of TCF7L2 repression may differ between stromal cells and myogenic cells.

DISCUSSION

The study of the heterogeneity of tissue-resident mesenchymal stromal populations emerges as an attractive field to underpin regeneration versus degenerative fibrosis (Mahmoudi et al., 2019; Lemos and Duffield, 2018; Lynch and Watt, 2018). Central to this idea is that different MSC populations and their lineage may have intrinsic properties that favor either permanent scar formation or regeneration via scar regression (Driskell et al., 2013; Malecova et al., 2018; Plikus et al., 2017; Rinkevich et al., 2015; Rognoni et al., 2018; Soliman et al., 2019 preprint; Furtado et al., 2016). Thus, investigating different sub-populations of fibroblasts, with particular niches and genetic programs, is important to understand how these cells and their progeny influence wound healing and tissue repair.

Here, we first reported differential gene expression of the four Tcf/Lef members in MSCs from skeletal muscle and cardiac tissue, MSCs, and MEFs. Second, using a combination of several methodologies and analyses, we established that TCF7L2 is a novel TGF-β target gene. Therefore, the gene and protein expression of TCF7L2 is strongly reduced by TGF-β signaling (Fig. 8). Conversely, the expression of several Wnt-dependent TCF7L2 target genes was impaired in response to TGF-β. Third, we showed via TCF7L2 BioGRID-based interaction network, *in silico* prediction of ubiquitination sites, and proteasome inhibition that TGF-β regulates TCF7L2 protein stability via the ubiquitin-proteasome system (Fig. 8). Mechanistically, we also described that HDACs inhibitors counteracted TGF-β-mediated repression of TCF7L2 expression in MSCs and fibroblasts (Fig. 8). Finally, we observed that TGF-β-driven TCF7L2 downregulation is MSCs specific, as this effect did not occur in TGF-β-stimulated C2C12 myoblasts. Taken together, our results suggest that the canonical Wnt pathway might participate through TCF7L2 in MSCs fate determination and the development of fibrosis, and therefore, this transcription factor emerges as a potential new target for the treatment of progressive degenerative diseases where chronic damage and fibrosis are common factors.

Like other high-mobility group box-containing proteins, Tcf/Lef act as activators or repressors of gene transcription mostly depending on their binding cofactors, activators or repressor and in a tissue- and cell-specific form (Frietze et al., 2012; Jin, 2016; Lien and Fuchs, 2014; Tang et al., 2008; Weise et al., 2010). Transcription factor 7-like 2 emerges as an interesting Tcf/Lef member to study because $TCF7L2^{+}$ MSCs are increased in fibrotic muscles from the *mdx* mice as well as in DMD patients (Contreras et al., 2016;

Pessina et al., 2015), and also in damaged muscles of the symptomatic amyotrophic lateral sclerosis (ALS) transgenic mice $hSOD^{G93A}$ (Gonzalez et al., 2017). Interstitial $TCF7L2^{+}$ fibroblasts also expand upon acute injury with Barium chloride in skeletal muscle (Murphy et al., 2011). $TCF7L2^{+}$-stromal cells peak at day 5 following injury and then return to their basal levels once the damage is resolved (Murphy et al., 2011). In addition, TCF7L2 is a transcriptional regulator in several cancers (Clevers, 2006; Cosin-Roger, 2019; Jin, 2016; Ravindranath et al., 2008; Tang et al., 2008; van de Wetering et al., 2002), and represents the gene more closely associated with risk of diabetes type 2 to date (Grant et al., 2006; Jin, 2016). Nevertheless, most of the knowledge concerning canonical Wnt signaling comes from β-Catenin translocation to the nucleus or dysregulated activity of upstream β-Catenin-stability regulators, but the precise contribution of Tcf/Lef to fibrogenesis has not been addressed yet.

Even though TCF7L2 was initially described as a marker for CT fibroblasts (Kardon et al., 2003; Mathew et al., 2011; Merrell et al., 2015), increasing evidence suggests that CT fibroblasts shared many cell properties with FAPs (Contreras et al., 2019b; Malecova et al., 2018; Wosczyna and Rando, 2018). A recent report demonstrates that TCF7L2 protein but not mRNA levels are increased during adipocyte differentiation, thereby TCF7L2 plays a regulatory role in fibroblast-adipocyte fate decisions *in vitro* and *in vivo* (Chen et al., 2018). In agreement with Chen and Cols. (2018), and contrary to what we found for TGF-β-mediated myofibroblast differentiation where *Tcf7l2* gene expression was repressed, we did not find *Tcf7l2* gene expression changes after adipogenic differentiation but increased *Tcf7l2* mRNA levels after osteogenic differentiation. The results presented above suggest that different MSC sub-populations (expressing different levels of TCF7L2) participate in the regenerative process after damage (Malecova et al., 2018). However, the precise role of TCF7L2 in fibroblast fate and decisions still needs to be addressed.

It is important to mention that our work may have some experimental limitations. For example, we have not explored the role of different Tcf/Lef members on the fate of MSCs yet. Here, we also reported that Tcf7l1 (Tcf3) is a Tcf/Lef gene with high expression in MSCs and fibroblasts. The regulation of the expression of Tcf7l1 seems to resemble that of Tcf7l2 but its role in FAPs and/or fibroblast biology still need to be further addressed. Interestingly, Tcf7 and Lef1 were expressed at very low levels in resting conditions, but they were strongly upregulated by TGF-β. This might be explained as a

compensatory regulatory mechanism of the Tcf/Lef family or as an independent response to TGF-β stimulation. However, this question needs to be addressed. On the other hand, Tcf7 and Lef1 are target genes of Tcf7l2 (Frietze et al., 2012; Lien et al., 2014), which may explain why these two members are upregulated when TCF7L2 is downregulated by TGF-β. Therefore, future studies need to address the questions raised above.

During the last two decades, the UPS has emerged as an essential component in cell and molecular biology via regulation of the cellular proteostasis in homeostasis and disease (Nalepa et al., 2006; Yuan et al., 2018). Therefore, we showed in this study the participation of the ubiquitin-proteasome system and deubiquitinase enzyme USP7 in the regulation of TCF7L2 steady-state levels and stability in response to TGF-β. Since deubiquitinases are upstream of the proteasome, their studies have drawn interest as drug targets (Yuan et al., 2018). We described that TCF7L2 protein half-life was about 3.5 h, and although, we did not address the ubiquitination status of TCF7L2, to our knowledge this is the first study suggesting potential cross-modulation between TGF-β and Wnt through deubiquitinating enzymes and the ubiquitin-proteasome system. TCF7L1 half-life was reported to be longer than 12 h, where the DNA-binding of TCF7L1 regulates its protein stability, and therefore, Wnt signaling (Shy et al., 2013). Since TGF-β signaling is a known chromatin-modifying factor (Massagué, 2012), an intriguing possibility is that DNA-binding of TCF7L2 regulates its stability and that TGF-β-induced chromatin remodeling might negatively affect TCF7L2 stability. Post-translational modifications of TCF7L2 occur at the phosphorylation level (Ishitani et al., 2003), acetylation (Elfert et al., 2013), and SUMOylation (Yamamoto et al., 2003). Although recent reports demonstrated the ubiquitination of Tcf/Lef (Han et al., 2017; Song et al., 2018, Yamada et al., 2006), the importance and extent of ubiquitination and ubiquitin-mediated regulatory mechanisms for Tcf/Lef TF activity are still elusive. Moreover, the complexity of different molecular events maintaining TCF7L2 protein or mRNA levels in proliferating FAPs and/or MSCs remains unclear. One limitation of this study is that we did not investigate the role of TCF7L2 in TGF-β-mediated extracellular matrix remodeling and myofibroblast differentiation. As TCF7L2 TF is known for regulating the expression of thousands of genes in a cell-type-specific manner (Frietze et al., 2012; Schuijers et al., 2014; Tang et al., 2008; Weise et al., 2010), we propose that TGF-β-induced TCF7L2 TF downregulation should have a massive and profound impact on stromal cells gene expression and molecular program. Here, we established that TGF-β impairs TCF7L2 expression and function in mesenchymal

549 progenitors but not in myoblasts. These results suggest that myoblasts could lack a
550 TCF7L2 regulatory program in response to TGF-β signaling that is present in fibroblasts.
551
552 Canonical Wnt signaling activation through Wnt-1 upregulates collagen ECM
553 deposition and promotes fibroblast differentiation into myofibroblast (Akhmetshina et al.,
554 2012). Similarly, TGF-β activates canonical Wnt cascade by inducing β-Catenin nuclear
555 accumulation and increasing Tcf/Lef-responsive elements activity in reporter assays, and
556 therefore, TGF-β mediates the reduction of the expression of the Wnt inhibitor DKK-1
557 (Akhmetshina et al., 2012). Also, pharmacological inhibition of Wnt/β-catenin signaling by
558 a small molecule, ICG-001, reduced the proliferation and TGF-β1-induced myofibroblast
559 actions of lung resident MSCs *in vitro* and exerted protective organ effects via attenuation
560 of bleomycin-induced lung fibrosis *in vivo* (Cao et al., 2018). These seminal studies and
561 others suggest that canonical Wnt cascade is required for TGF-β-mediated fibrosis, and
562 vice versa (Cosin-Roger et al., 2019; Działo et al., 2018; Piersma et al., 2015). Based on
563 our results we suggest that TGF-β signaling plays a regulatory role in TCF7L2 expression
564 and function that, in mesenchymal cells, could be acting as a negative profibrotic loop.
565 Hence, we hypothesize that extracellular TGF-β release in the stromal space after injury
566 primes progenitor cells to differentiate toward TCF7L2 non-expressing myofibroblasts,
567 which are then refractory to the self-renewal Wnt signals. Central to this idea is the
568 significance of restraining an exacerbated stromal response to control scar formation.
569 Thus, Wnt/TCF7L2 and TGF-β signaling could interact in a cell-specific and complex
570 arrangement during regeneration and repair. Wnt cascade through Tcf/Lef TFs might
571 crosstalk with TGF-β signaling during the progression of the pathology, by regulating the
572 survival of MSCs, their cell fate determination, and ECM gene expression. However,
573 further studies are needed to fully address this question and to completely understand the
574 role of each Tcf/Lef TF during scar-formation.
575
576 A complex array of different signals regulates FAP activation and persistence in the
577 tissue milieu. TNF-α promotes FAP apoptosis, while TGF-β induces both FAP expansion
578 and survival following damage (Lemos et al., 2015; Uezumi et al., 2011). Conversely,
579 TGF-β mediates the differentiation of FAPs into myofibroblasts at the expense of
580 adipogenic differentiation (Contreras et al., 2019c; Uezumi et al., 2014a; Uezumi et al.,
581 2011). To date, the role of TNF-α signaling, or other relevant signaling pathways that
582 control muscle regeneration, in Tcf7l2 expression has not previously been reported.

583 Dynamic regulation of stromal and/or fibroblast markers following damage has been also
584 identified in resident stromal cardiac fibroblasts (Farbehi et al., 2019; Kanisicak et al.,
585 2016; Tallquist and Molkentin, 2017) and skeletal muscle (Contreras et al., 2019c;
586 Malecova et al., 2018; Petrilli et al., 2017 preprint; Soliman et al., 2019 preprint). We have
587 recently reported that the *in vivo* and *in vitro* expression of PDGFRα is strongly
588 downregulated by damage-associated TGF-β signaling in skeletal muscle and heart
589 mesenchymal stromal cells (Contreras et al., 2019c). In summary, the work of others and
590 our results suggest that stromal stem cell and/or progenitor markers are often
591 downregulated by TGF-β and probably after a complex array of niche signals during
592 regeneration or disease, as cells change phenotypically towards an activated ECM-
593 producing cell or myofibroblast. These downregulated stromal and/or fibroblast markers
594 include Sca-1, PDGFRα, and Tcf21 (Asli et al., 2018 preprint; Contreras et al., 2019c; Fu
595 et al., 2018; Kanisicak et al., 2016; Petrilli et al., 2017 preprint; Soliman et al., 2019
596 preprint). With our work, we added Tcf7l2 to the growing list. The *in vivo* cause-effect of
597 this cell-type-specific marker downregulation and the physiological extent of this
598 phenomenon needs to be further investigated in a cell- and tissue-specific manner.
599
600 In the last two decades, our understanding of the cellular and molecular
601 determinants of fibrosis has advanced immensely (Ceco and McNally, 2013; Kim et al.,
602 2018; Piersma et al., 2015; Smith and Barton, 2018). Nevertheless, the lack of successful
603 antifibrotic therapy to date prompts us to continue the search for new potential candidates
604 to fight against non-malignant proliferative disorders. Compelling evidence from this work
605 raises the notion that TCF7L2 should be explored as a therapeutic target in fibrotic
606 diseases, as Wnt β/Catenin pathway emerges as a novel and attractive cascade to target
607 for improving organ function during tissue fibrosis (Xiang et al., 2017). Although our
608 knowledge about mesenchymal stromal progenitor cell biology has exploded in the past
609 decade, we still lack information about the origin, self-renewal, gene regulation,
610 epigenetics, aging, and senescence of these remarkable cells. The identification of
611 signaling pathways and molecular programs that regulate stromal cell activity to promote
612 muscle regeneration without degenerative scar-tissue should offer great therapeutic
613 benefits for myopathies, fibrosis-related disorders, and aging.

MATERIALS AND METHODS

Mice and study approval

Housing, husbandry and experimental protocols were conducted in strict accordance and with the formal approval of the Animal Ethics Committee of the Pontificia Universidad Católica de Chile (Doctoral ID protocol: 160512005) and following institutional and national guidelines at the University of British Columbia, Canada. Mice were housed in standard cages under 12-h light-dark cycles and fed *ad libitum* with a standard chow diet. Five-month-old C57BL/10ScScJ male mice (hereafter referred to as wild type, WT; stock #000476) and dystrophic C57BL/10ScSn-Dmdmdx/J mice (stock #001801) male mice (both from Jackson Laboratories) were used in experiments for Fig. 1E, Fig. 2, and Fig. S2H. *Pdgfra*$^{tm11(EGFP)Sor}$ mice (hereafter referred to as PDGFRα^{H2BEGFP} mice) were purchased from Jackson Laboratories (stock #007669 B6.129S4-Pdgfra$^{tm11(EGFP)Sor}$/J; Hamilton et al., 2003). For FAP detection in *mdx* muscles, we crossed male C57Bl/10ScSn-*mdx* mice with hemizygous female B6.129S4-Pdgfra$^{tm11(EGFP)Sor}$/J mice. We used the F1 male *mdx*;PDGFRα^{H2BEGFP} offspring (5- to 6-month-old), and the comparisons were performed among siblings. All surgeries were performed after the mice had been anesthetized with 2.5–3% of isoflurane gas in pure oxygen. The mice were euthanized with cervical dislocation at the ages indicated in each figure, and the tissues were immediately processed, either by direct freezing in liquid nitrogen for protein and RNA extraction or in 2-methyl butane cooled with liquid nitrogen for histological analysis as described below.

Muscle acute injury

For acute glycerol injury, the tibialis anterior (TA) muscle of 2- to 3-monthold PDGFRα^{H2BEGFP} mice was injected with 50 µl 50% v/v glycerol. Tissue collection was performed as indicated in the corresponding figures after glycerol injections. Notexin muscle damage was induced by intramuscular injection of 0.15 µg notexin snake venom (Latoxan) into the TA muscle (Contreras et al., 2019c; Joe et al., 2010; Lemos et al., 2015). Non-injected muscles from the contralateral limb were used as a control. Muscles were isolated and collected for analysis at the indicated time points in the corresponding figures.

Tissue preparation, flow cytometry and FACS

Tissue preparation for skeletal muscle and heart FAPs was performed mainly as described before (Contreras et al., 2019c; Judson et al., 2017; Soliman et al., 2019 preprint). One-step digestion of tissue for FAPs was performed mainly as described before with some modifications (Judson et al., 2017; Lemos et al., 2015). All the steps were performed on ice unless otherwise specified. Briefly, skeletal muscle from both hindlimbs (limb FAPs), and diaphragm (diaphragm FAPs) was carefully dissected, washed with 1×PBS, cut into small pieces with scissors until homogeneous. Collagenase D (Roche Biochemicals) 1.5 U/ml and Dispase II (Roche Biochemicals) 2.4 U/ml, in 2.5 mM CaCl2, was added to every two hindlimbs in a total volume of 3 ml per mouse, and the preparation was placed at 37°C for 45 min with rotation. Preparations were passed through a 70 µm, and then 40 µm cell strainer (Becton Dickenson), and washed with FACS buffer (PBS, 2% FBS, 2 mM EDTA pH 7.9). Resulting single cells were collected by centrifugation at 1000 *g* for 5–10 min. Cell preparations were incubated with primary antibodies for 20–30 min at 4°C in FACS buffer at ~3×107 cells/ml.We used the following monoclonal primary antibodies: anti-CD31 (clones MEC13.3, Cat. no. 553372, Becton Dickenson; clone 390, Cat. no. CL8930F-3, 1:500, Cedarlane Laboratories), anti-CD45 (clone 30-F11, Cat. no. 557659, 1:400, Becton Dickenson), anti-CD45.1 (1:400; clone A20, Cat. no. 553775, 1:400, Becton Dickenson), anti-CD45.2 (clone 104, Cat. no. 11-0454-85, eBiosciences), anti-Sca-1 (1:2000–1:5000; clone D7, Cat. no. 25-5981-82, Invitrogen) and anti-α7 integrin (1:11500; Clone R2F2, Cat. no. 67-0010-05, AbLab). For all antibodies, we performed fluorescence minus one control by staining with appropriate isotype control antibodies (rat IgG2a kappa, PE-Cyanine7, clone eBR2a, Cat. no. 25-4321-82, eBioscience. 1:400; mouse anti-IgG2a k, FITC, clone G155-178, BD, Cat No: 553456; rat IgG2b kappa, APC, clone eB149/10H5, Cat. no. 17-4031-82 – all from eBioscience). To assess viability, cells were stained with propidium iodide (1 µg ml–1) and Hoechst 33342 (2.5 µg ml–1) and resuspended at ~1×106 cells ml–1 immediately before sorting or analysis. The analysis was performed on a LSRII (Becton Dickenson) flow cytometer equipped with three lasers. Data were collected using FacsDIVA software. Cell sorting was performed on a FACS Vantage SE (Becton Dickenson), BD Influx flow cytometer (Becton Dickinson), or FACS Aria (Becton Dickenson), all equipped with three lasers, using a 100-µm nozzle at 18 psi to minimize the effects of pressure on the cells. Sorting gates were strictly defined based on isotype control (fluorescence minus one) stains. All flow cytometry data were analyzed using FlowJo 10.5.3v.

Reagents

The TGFBR1 inhibitor SB525334 (used at 5 μM; S8822, Sigma-Aldrich), p38 MAPK SB203580 inhibitor (used at 20 μM; 5633, Cell Signaling Technology), PI3K/AKT inhibitor LY294002 (used at 10 μM; 440202, Merck-Calbiochem), the inhibitor of MEK1/2/ERK1/2 kinases UO126 (used at 10 μM; 9903, Cell Signaling Technology), Smad3 inhibitor SIS3 (used at 6 μM; 1009104-85-1, Merck-Calbiochem), the inhibitor of JNK activity SB600125 (used at 20 μM; Cell Signaling Technology), trichostatin A (TSA) (used at 10 μM; T8552, Sigma-Aldrich), and the inhibitor of USP7 activity HBX 41108 (used at 10uM; 4285; Tocris) were all diluted in DMSO. DMSO alone was used as a control. Cycloheximide (C104450, Sigma-Aldrich) was diluted in ethanol and used at 30μg/ml final concentration. All the inhibitors used were added at the same time and co-incubated with TGF-β1. Other reagents, unless otherwise is indicated, were purchased from Sigma-Aldrich.

Cell culture and nuclei cytoplasmic fractionation

The murine mesenchymal stromal cell (MSC) cell line C3H/10T1/2, Clone 8, and the embryonic fibroblast cell line NIH-3T3 were obtained from American Type Culture Collection (ATCC) and grown at 37°C in 5% CO2 in growth medium (GM): high-glucose Dulbecco's modified Eagle's medium (DMEM) (Invitrogen) with 10% fetal bovine serum (FBS; Hyclone) and supplemented with antibiotics (Gutiérrez et al., 2015). The murine C2C12 myoblast cell line (American Type Culture Collection (ATCC), VA, USA) were cultured at 37 °C in 8% CO2 in growth medium (GM); DMEM high glucose (Invitrogen, CA, USA) with 10% fetal bovine serum (FBS) (Hyclone, UT, USA) and supplemented with antibiotics. Cells were treated with recombinant hTGF-β1 (#580702, Biolegend, USA), recombinant hTGF-β2 (#583301, Biolegend, USA), recombinant hTGF-β3 (#501123524, eBioscience, CA, USA) in Dulbecco's modified Eagle's medium (DMEM) supplemented with 2% (v/v) FBS and penicillin/streptomycin in a 5% CO2 atmosphere at concentration and time indicated in the corresponding figure legend. Adipogenic or osteogenic differentiation of MEFs was induced for 28 days with MesenCult™ Adipogenic Differentiation Kit (Mouse) (STEMCELL Technologies, Canada) and MesenCult™ Osteogenic Stimulatory Kit (Mouse), respectively. Our cell cultures were periodically tested to ensure no mycoplasma contamination using polymerase chain reaction (PCR). Cell fractionation was performed mainly according the principles of rapid, efficient and practical (REAP) method for subcellular fractionation with a few modifications (Suzuki et al., 2010). Briefly, the initially PBS-scraped and pelleted cells were resuspended, by pipetting

up/down and vortexing for 5 sec, using 900 µL of "cytoplasmic buffer": 10mM Tris pH 7.5, 3mM $MgCl_2$, 100mM $NaCl_2$, 1mM EGTA, 0.25% (v/v) Nonidet P-40. Next, 300 µL of the initial lysate was removed and kept as "whole cell lysate". The remaining (~600 µL) material was centrifuged for 10 sec (two times) in 1.5 ml micro-centrifuge tubes and 300 µL of the supernatant was removed and kept as the "cytosolic fraction". After the remaining supernatant was removed, the pellet (~20 µL) was resuspended with 180 µL of 1 × Laemmli sample buffer and designated as "nuclear fraction". 100 µL of 4 x Laemmli sample buffer was added to both the whole cell lysate and the cytosolic fractions. Finally, samples were sonicated and 30 µL, 30 µL and 15 µL of whole cell lysate, cytoplasmic and nuclear fractions, respectively, were loaded and electrophoresed using sodium dodecyl sulfate polyacrylamide gel electrophoresis (SDS-PAGE) (see below).

FAP cell culture

FAPs were FACS sorted from either wild-type or PDGFRα$^{H2BEGFP/+}$ mice and grown in high-glucose DMEM (Invitrogen), supplemented with 10% FBS, 1% sodium pyruvate, and 2.5 ng/ml bFGF (Invitrogen) at a density of 15,000 cell/cm^2 in a 48-well plate or 24-well plate. Cells were isolated from undamaged muscles. For the TGF-β1 treatment experiment, after 72 h to 96 h in culture and 70–80% confluence, FAPs were stimulated with 5 ng/ml TGF-β1 (Contreras et al., 2019b). Cells were then collected for further analyses.

Protein extraction and western blot analysis

Protein extracts from cells were obtained using RIPA 1x lysis buffer (9806, Cell Signaling, MA, USA) plus protease/phosphatase inhibitors (#P8340/#P0044, Sigma-Aldrich, USA). The cells were sonicated for 10 s and centrifuged at 9,000 *g*. Proteins were quantified with the Micro BCA assay kit, following the manufacturer's instructions (Pierce, IL, USA). Extracts were subjected to SDS-PAGE electrophoresis in 9-10% (or 12% in Fig. S6B) polyacrylamide gels, transferred to PDVF membranes (Millipore, CA, USA), and probed with primary antibodies: goat anti-PDGFRα (1:1000; AF1062, R&D Systems), rabbit anti-TCF4/TCF7L2 (C48H11) (1:1000; 2569, Cell Signaling), rabbit anti-c-Jun (60A8) (1:1000; 9165, Cell Signaling), rabbit anti-β-Catenin (1:2000; 9562, Cell Signaling), rabbit anti-histone 3 H3 (1:1000; 9715, Cell signaling), mouse anti-alpha smooth muscle actin (αSMA) (1:2000; A5228, Sigma-Aldrich, St. Louis, MO, USA), goat anti-CCN2/CTGF (1;500; Cat. no. sc-14939, Santa Cruz Biotechnology), rabbit anti-Integrin β1 (M-106) (1:1000; sc-8978, Santa Cruz Biotechnology), rabbit anti-fibronectin (1:2000; F3648,

Sigma-Aldrich), mouse anti-Myosin Skeletal Fast (1:1000; M4276, Sigma-Aldrich), rabbit anti-myogenin (1:500; sc-576, Santa Cruz), mouse anti-GAPDH (1:5000; MAB374, Millipore), mouse anti-α-tubulin (1:5000; T5168, Sigma-Aldrich), Then, primary antibodies were detected with a secondary antibody conjugated to horseradish peroxidase: mouse anti-goat IgG (1:5000; 31400), goat anti-rabbit IgG (1:5000; 31460) and goat anti-mouse IgG (1:5000; 31430), all from Pierce. All immunoreactions were visualized by enhanced chemiluminescence Super Signal West Dura (34075, Pierce) or Super Signal West Femto (34096, Pierce) by a ChemiDoc-It HR 410 imaging system (UVP). Western blot densitometry quantification was done using Fiji
software (ImageJ version 2.0.0-rc/69/1.52n). Briefly, minimum brightness thresholds were increased to remove background signal. Remaining bands were bracketed, plot profiles generated, and area under histograms auto traced. Protein levels were normalized with the levels of the loading control. Ponceau S Red Staining Solution (0.1% (w/v) Ponceau S in 5% (v/v) acetic acid) was used.

Indirect immunofluorescence and microscopy

Cells immunofluorescence was performed as previously described (Contreras et al., 2018). For tissue section immunofluorescence, flash-frozen muscles were sectioned at 7 µm, fixed for 15 min in 4 % paraformaldehyde, and washed in phosphate-buffered saline (PBS). Cells and tissue sections were blocked for 30–60 min in 1 % bovine serum albumin (BSA) plus 1 % fish gelatin in PBS, incubated overnight at 4 °C in primary antibody: rat anti-Laminin-α2 (L0663, Sigma-Aldrich), mouse anti-alpha smooth muscle actin (αSMA) (1:250) (Sigma-Aldrich, St. Louis, MO, USA). Then, washed in PBS, incubated for 1 h or at room temperature with a secondary antibody and washed in PBS. Hoechst 33342 stain (2 mg/ml) and wheat germ agglutinin (WGA) Alexa Fluor 594 conjugate (#W11262, Invitrogen, CA, USA) were added for 10 min in PBS before the slides were mounted, according to the supplier's instructions. Slides were then washed in PBS and mounted with fluorescent mounting medium (DAKO, USA). To stain F-actin Alexa Fluor 568 Phalloidin was added to the cells according to provider's instructions for 10 minutes (#A12380, Thermo-Fisher, MA, USA). Cells were imaged on a Nikon Eclipse C2 Si Confocal Spectral Microscope or Nikon Eclipse Ti Confocal Microscope using Nikon NIS-Elements AR software 4.00.00 (build 764) LO, 64 bit. Confocal images were acquired at the Unidad de Microscopía Avanzada (UMA), Pontificia Universidad Católica de Chile, using a Nikon Eclipse C2 Si confocal spectral microscope. Plan-Apochromat objectives were used

(Nikon, VC 20× DIC N2 NA 0.75, 40× OIL DIC H NA 1.0, and, VC 60× OIL DIC NA 1.4). Cytospin confocal microscopy was performed using a Nikon eclipse Ti Confocal Microscope with a C2 laser unit. Confocal microscopy images shown in Fig. 1G, Fig. 2C and Fig. S1G were composed using maximum-intensity projection z-stack reconstructions (0.3 µm each stack) of 7-µm-thick transversal sections or cultured cells. Then, we automatically analyzed the intensity of fluorescence (amount) of TCF7L2 in TCF7L2^{+} cells using the analyze particles plugging, and manually counted the cells using the cell counter plugging from Fiji software (ImageJ version 2.0.0-rc/69/1.52n, NIH). Counts of 4–8 randomly chosen fields and mild and severe damage fields were averaged from four independent experiments.

RNA isolation, reverse transcription, and quantitative real-time polymerase chain reaction (RT-qPCR)

Total RNA from cultured cells was isolated using TRIzol (Invitrogen, CA, USA) according to the manufacturer's instructions. RNA integrity was corroborated as described before (Contreras et al., 2018). Two microgram RNA was reverse transcribed into cDNA using random primers and M-MLV reverse transcriptase (Invitrogen, CA, USA). RT-qPCR was performed in triplicate with the Eco Real-Time PCR System (Illumina, CA, USA), using primer sets for (Supp Table 1): *Tcf7*, *Lef1*, *Tcf7l1 (Tcf3)*, *Tcf7l2 (Tcf4)*, *Ccn2/Ctgf*, *Fibronectin (Fn), Periostin*, *(Postn)*, *Integrin aV (IntαV)*, *Collagen 6a1 (Col6a1)*, *Collagen 6a3 (Col6a3)*, *Integrin b1 (Intβ1)*, *Adiponectin (Adipoq), c/EBP*, *Pparg.*, and the housekeeping gene *18s* (used as a reference gene). The ΔΔCt method was used for quantification, and mRNA levels were expressed relative to the mean level of the control condition in each case. We analyzed and validated each RT-qPCR expected gene product using a 2% agarose gel. Digital droplet PCR was performed as previously described (Soliman et al., 2019 preprint). Gene expression analysis was performed using Taqman Gene Expression Assays (Applied Biosystems), on a 7900HT Real Time PCR system (Applied Biosystems). Sequence information for the primers contained in the Taqman assays is provided here: Taqman probes (Thermo Fisher Scientific): Tcf7l2 mouse (Mm00501505_m1), Tcf7l1 mouse (Mm01188711_m1), Lef1 mouse (Mm00550265_m1), Tcf7 mouse (Mm00493445_m1), Runx2 mouse (Hs01047973_m1), Adipoq (Hs00605917_m1), and the housekeeping gene *Hprt* mouse (Mm03024075_m1). Data were acquired and analyzed using SDS 2.0 and SDS RQ Manager software (Applied Biosystems).

817

818 **Computational BioGRID database, Ubiquitination, and Tabula Muris open source**
819 **database**

820 The image in Fig. 6D was generated with BioGRID based on human TCF7L2 interactome
821 (Stark et al., 2006). The data from figures and tables in the BioGRID webpage
822 (https://thebiogrid.org/) can be searched and sorted. For post-translational modification
823 detection and delineation of ubiquitination at a site-specific level we used UbiSite webpage
824 (http://csb.cse.yzu.edu.tw/UbiSite/) (Akimov et al., 2018). Murine Tabula Muris open
825 database was used to generate the figures shown in Fig. S1E,F (The Tabula Muris
826 Consortium et al., 2018). Data were extracted and analyzed from total tissues, diaphragm,
827 and limb muscles.

828

829 **Statistical analysis**

830 Mean ± s.e.m. values, as well as the number of experiments performed, are indicated in
831 each figure. All datasets were analyzed for normal distribution using the D'agostino
832 normality test. Statistical significance of the differences between the means was evaluated
833 using the one-way analysis of variance (ANOVA) test followed by post-hoc Dunnett's
834 multiple comparison test and the significance level set at $P<0.05$. A two-tailed Student's *t*-
835 test was performed when two conditions were compared. Differences were considered
836 significant with $P<0.05$. Data were collected in Microsoft Excel, and statistical analyses
837 were performed using Prism 8 software for macOS (GraphPad).

Acknowledgments

We are grateful to the Unidad de Microscopía Avanzada (UMA) of Pontificia Universidad Católica de Chile for its support in image acquisition. We acknowledge the services provided by the UC CINBIOT Animal Facility funded by the PIA CONICYT* ECM-07 Program for Associative Research, of the Chilean National Council for Science and Technology. We also acknowledge the animal unit staff and genotyping core facility at the Biomedical Research Centre (UBC), especially Mr Taka Murakami, Mrs Krista Ranta and Mr Wei Yuan. We thank Mr Andy Johnson and Mr Justin Wong of UBC Flow Cytometry. We also acknowledge Martin Arostegui from Michael Underhill's Lab (Biomedical Research Centre, UBC) for helping with MEFs culture. We acknowledge the Hugo Olguín Lab (Pontificia Universidad Católica de Chile) for kindly providing USP7 small-molecule inhibitor HBX 41108. For administrative assistance, we thank Ms Vanessa Morales and Ms Vittoria Canale. We also acknowledge Mr. Eduardo Ramirez and Ms Darling Vera for their technical support.

Funding

Fondo Nacional de Desarrollo Científico y Tecnológico (FONDECYT) grant 1190144 and Comisión Nacional de Investigación Científica y Tecnológica (CONICYT) grant AFB170005 to E.B.; CONICYT Beca de Doctorado Nacional Folio 21140378 to O.C.; and Canadian Institutes of Health Research (CIHR) grant FDN-159908 to F.M.R. supported this work. The funding agencies had no role in the design of the study, data collection, analysis, the decision to publish or preparation of the manuscript.

Availability of data and materials

All data generated or analyzed during this study are included in this published article.

Authors' contributions

Conceptualization: O.C., E.B.; Methodology: O.C., H.S., M.T.; Software: O.C.; Validation: O.C., H.S., M.T., F.M.R., E.B.; Formal analysis: O.C., H.S.; Investigation: O.C., H.S., M.T.; Resources: O.C., F.M.R., E.B.; Data curation: O.C.; Writing - original draft: O.C.; Writing - review & editing: O.C., H.S., M.T., F.M.R., E.B.; Visualization: O.C., H.S., M.T., F.M.R., E.B.; Supervision: O.C., F.M.R., E.B.; Project administration: O.C., E.B.; Funding acquisition: O.C., E.B., F.M.R.

Ethics approval and consent to participate

Not applicable.

Consent for publication

Not applicable.

Competing interests

The authors declare that they have no competing financial interests.

References

Aberle, H., Bauer, A., Stappert, J., Kispert, A., & Kemler, R. (1997). β-catenin is a target for the ubiquitin–proteasome pathway. *The EMBO Journal*, 16(13), 3797–3804. https://doi.org/10.1093/emboj/16.13.3797

Accornero, F., O. Kanisicak, A. Tjondrokoesoemo, A.C. Attia, E.M. McNally, and J.D. Molkentin. 2014. Myofiber-specific inhibition of TGFbeta signaling protects skeletal muscle from injury and dystrophic disease in mice. *Hum Mol Genet*. 23:6903-6915.

Acuña, M.J., P. Pessina, H. Olguin, D. Cabrera, C.P. Vio, M. Bader, P. Munoz-Canoves, R.A. Santos, C. Cabello-Verrugio, and E. Brandan. 2014. Restoration of muscle strength in dystrophic muscle by angiotensin-1-7 through inhibition of TGF-beta signalling. *Hum Mol Genet*. 23:1237-1249.

Agley, C. C., Rowlerson, A. M., Velloso, C. P., Lazarus, N. R., & Harridge, S. D. R. (2013). Human skeletal muscle fibroblasts, but not myogenic cells, readily undergo adipogenic differentiation. *Journal of Cell Science*, 126(24), 5610 LP – 5625. https://doi.org/10.1242/jcs.132563

Akimov, V., Barrio-Hernandez, I., Hansen, S. V. F., Hallenborg, P., Pedersen, A.-K., Bekker-Jensen, D. B., … Blagoev, B. (2018). UbiSite approach for comprehensive mapping of lysine and N-terminal ubiquitination sites. *Nature Structural & Molecular Biology*, 25(7), 631–640. https://doi.org/10.1038/s41594-018-0084-y

Asli, N. S., Xaymardan, M., Patrick, R., Farbehi, N., Cornwell, J., Forte, E., … Harvey, R. P. (2019). PDGFRα signaling in cardiac fibroblasts modulates quiescence, metabolism and self-renewal, and promotes anatomical and functional repair. *BioRxiv*, 225979. https://doi.org/10.1101/225979

Burgy, O., & Königshoff, M. (2018). The WNT signaling pathways in wound healing and fibrosis. *Matrix biol*, 68–69, 67–80. https://doi.org/https://doi.org/10.1016/j.matbio.2018.03.017

Bernasconi, P., C. Di Blasi, M. Mora, L. Morandi, S. Galbiati, P. Confalonieri, F. Cornelio, and R. Mantegazza. 1999. Transforming growth factor-beta1 and fibrosis in congenital muscular dystrophies. *Neuromuscul Disord*. 9:28-33.

Biressi, S., Miyabara, E. H., Gopinath, S. D., Carlig, P. M. M., & Rando, T. A. (2014). A Wnt-TGF2 axis induces a fibrogenic program in muscle stem cells from dystrophic mice. *Science Translational Medicine*. https://doi.org/10.1126/scitranslmed.3008411

Bolden, J. E., Peart, M. J., & Johnstone, R. W. (2006). Anticancer activities of histone deacetylase inhibitors. *Nature Reviews Drug Discovery*, 5(9), 769–784. https://doi.org/10.1038/nrd2133

Brack, A. S., Conboy, M. J., Roy, S., Lee, M., Kuo, C. J., Keller, C., & Rando, T. A. (2007). Increased Wnt signaling during aging alters muscle stem cell fate and increases fibrosis. *Science*. https://doi.org/10.1126/science.1144090

Braun, T., G. Buschhausen-Denker, E. Bober, E. Tannich, and H.H. Arnold. 1989. A novel human muscle factor related to but distinct from MyoD1 induces myogenic conversion in 10T1/2 fibroblasts. *EMBO J*. 8:701-709.

Burgy, O., & Königshoff, M. (2018). The WNT signaling pathways in wound healing and fibrosis. *Matrix biol*, 68–69, 67–80. https://doi.org/https://doi.org/10.1016/j.matbio.2018.03.017

Callahan, J.F., J.L. Burgess, J.A. Fornwald, L.M. Gaster, J.D. Harling, F.P. Harrington, J. Heer, C. Kwon, R. Lehr, A. Mathur, B.A. Olson, J. Weinstock, and N.J. Laping. 2002. Identification of novel inhibitors of the transforming growth factor beta1 (TGF-beta1) type 1 receptor (ALK5). *J Med Chem*. 45:999-1001.

Cao, H., Wang, C., Chen, X., Hou, J., Xiang, Z., Shen, Y., & Han, X. (2018). Inhibition of Wnt/β-catenin signaling suppresses myofibroblast differentiation of lung resident mesenchymal stem cells and pulmonary fibrosis. *Scientific Reports*, 8(1), 13644. https://doi.org/10.1038/s41598-018-28968-9

Carr, M. J., Toma, J. S., Johnston, A. P. W., Steadman, P. E., Yuzwa, S. A., Mahmud, N., … Miller, F. D. (2019). Mesenchymal Precursor Cells in Adult Nerves Contribute to Mammalian Tissue Repair and Regeneration. *Cell Stem Cell*, 24(2), 240-256.e9. https://doi.org/10.1016/j.stem.2018.10.024

Ceco, E., and E.M. McNally. 2013. Modifying muscular dystrophy through transforming growth factor-beta. *FEBS J*. 280:4198-4209.

Chen, X., Ayala, I., Shannon, C., Fourcaudot, M., Acharya, N. K., Jenkinson, C. P., … Norton, L. (2018). The Diabetes Gene and Wnt Pathway Effector TCF7L2 Regulates Adipocyte Development and Function. *Diabetes*, 67(4), 554 LP – 568. https://doi.org/10.2337/db17-0318

Chilosi, M. et al. Aberrant Wnt/beta-catenin pathway activation in idiopathic pulmonary fibrosis. *Am. J. Pathol*. 162, 1495–1502 (2003).

Cho, N., Razipour, S. E., & McCain, M. L. (2018). TGF-β1 dominates extracellular matrix rigidity for inducing differentiation of human cardiac fibroblasts to myofibroblasts. *Experimental Biology and Medicine*, 243(7), 601–612. https://doi.org/10.1177/1535370218761628

950 Cisternas, P., Henriquez, J. P., Brandan, E., & Inestrosa, N. C. (2014). Wnt Signaling in Skeletal Muscle
951 Dynamics: Myogenesis, Neuromuscular Synapse and Fibrosis. *Molecular Neurobiology*, 49(1), 574–589.
952 https://doi.org/10.1007/s12035-013-8540-5
953
954 Clevers, H., 2006. Wnt/β-Catenin Signaling in Development and Disease. *Cell* 127: 3, 469-480.
955
956 Cohn, R.D., C. van Erp, J.P. Habashi, A.A. Soleimani, E.C. Klein, M.T. Lisi, M. Gamradt, C.M. ap Rhys,
957 T.M.
958
959 Colland, F., Formstecher, E., Jacq, X., Reverdy, C., Planquette, C., Conrath, S., … Daviet, L. (2009). Small-
960 molecule inhibitor of USP7/HAUSP ubiquitin protease stabilizes and activates p53 in cells. *Molecular*
961 *Cancer Therapeutics*, 8(8), 2286 LP – 2295. https://doi.org/10.1158/1535-7163.MCT-09-0097
962
963 Holm, B.L. Loeys, F. Ramirez, D.P. Judge, C.W. Ward, and H.C. Dietz. 2007. Angiotensin II type 1 receptor
964 blockade attenuates TGF-beta-induced failure of muscle regeneration in multiple myopathic states. *Nat*
965 *Med*. 13:204-210.
966
967 Colwell, A. S., Krummel, T. M., Longaker, M. T. & Lorenz, H. P. Wnt-4 expression is increased in fibroblasts
968 after TGF-beta1 stimulation and during fetal and postnatal wound repair. *Plast. Reconstr. Surg*. 117, 2297–
969 2301 (2006).
970
971 Contreras, O., D.L. Rebolledo, J.E. Oyarzun, H.C. Olguin, and E. Brandan. 2016. Connective tissue cells
972 expressing fibro/adipogenic progenitor markers increase under chronic damage: relevance in fibroblast-
973 myofibroblast differentiation and skeletal muscle fibrosis. *Cell Tissue Res*. 364:647-660.
974
975 Contreras, O., M. Villarreal, and E. Brandan. 2018. Nilotinib impairs skeletal myogenesis by increasing
976 myoblast proliferation. *Skelet Muscle* **8**, 5. doi:10.1186/s13395-018-0150-5
977
978 Contreras O, Rebolledo D, Oyarzún J and Brandan E. Fibroblasts (Tcf4) and mesenchymal progenitors
979 (PDGFRα) correspond to the same cell type and are increased in skeletal muscle dystrophy, denervation
980 and chronic damage [version 1; not peer reviewed]. F1000Research 2019a, 8:299 (poster)
981 (https://doi.org/10.7490/f1000research.1116478.1)
982
983 Contreras, O., Rossi, F. M., & Brandan, E. (2019b). Adherent muscle connective tissue fibroblasts are
984 phenotypically and biochemically equivalent to stromal fibro/adipogenic progenitors. *Matrix Biology Plus*.
985 https://doi.org/https://doi.org/10.1016/j.mbplus.2019.04.003
986

Contreras, O., Cruz-Soca, M., Theret, M., Soliman, H., Tung, L. W., Groppa, E., Rossi, F. M. and Brandan, E. (2019c). Cross-talk between TGF-β and PDGFRα signaling pathways regulates the fate of stromal fibro–adipogenic progenitors. *Journal of Cell Science.* 132, 232157. https://doi.org/10.1242/JCS.232157

Cosin-Roger, J., Ortiz-Masià, M. D., & Barrachina, M. D. (2019). Macrophages as an Emerging Source of Wnt Ligands: Relevance in Mucosal Integrity. *Frontiers in Immunology*. Retrieved from https://www.frontiersin.org/article/10.3389/fimmu.2019.02297

Danna, N.R., B.G. Beutel, K.A. Campbell, and J.A. Bosco, 3rd. 2014. Therapeutic approaches to skeletal muscle repair and healing. *Sports Health*. 6:348-355.

David, C. J. and Massagué, J. (2018). Contextual determinants of TGFβ action in development, immunity and cancer. *Nat. Rev. Mol. Cell Biol.* **19**, 419-435. doi:10.1038/s41580-018-0007-0

Degirmenci, B., Hausmann, G., Valenta, T., & Basler, K. (2018). Chapter One - Wnt Ligands as a Part of the Stem Cell Niche in the Intestine and the Liver. In J. Larraín & G. B. T.-P. in M. B. and T. S. Olivares (Eds.), WNT Signaling in Health and Disease (Vol. 153, pp. 1–19). Academic Press. https://doi.org/https://doi.org/10.1016/bs.pmbts.2017.11.011

Derynck, R., & Budi, E. H. (2019). Specificity, versatility, and control of TGF-b family signaling. *Science Signaling*. https://doi.org/10.1126/scisignal.aav5183

Driskell, R. R., Lichtenberger, B. M., Hoste, E., Kretzschmar, K., Simons, B. D., Charalambous, M., Ferron, S. R., Herault, Y., Pavlovic, G., Ferguson-Smith, A. C. et al. (2013). Distinct fibroblast lineages determine dermal architecture in skin development and repair. *Nature* 504, 277-281. doi:10.1038/nature12783

Droguett, R., Cabello-Verrugio, C., Riquelme, C., & Brandan, E. (2006). Extracellular proteoglycans modify TGF-β bio-availability attenuating its signaling during skeletal muscle differentiation. *Matrix biol*. https://doi.org/10.1016/j.matbio.2006.04.004

Dulauroy S, Di Carlo SE, Langa F, Eberl G, Peduto L. Lineage tracing and genetic ablation of ADAM12(+) perivascular cells identify a major source of profibrotic cells during acute tissue injury. *Nature medicine*. 2012;18(8):1262–70. pmid:22842476

Działo, E., Tkacz, K., & Błyszczuk, P. (2018). Crosstalk between the TGF-β and WNT signalling pathways during cardiac fibrogenesis. Acta Biochimica Polonica. https://doi.org/10.18388/abp.2018_2635

Elfert, S., Weise, A., Bruser, K., Biniossek, M. L., Jägle, S., Senghaas, N., & Hecht, A. (2013). Acetylation of Human TCF4 (TCF7L2) Proteins Attenuates Inhibition by the HBP1 Repressor and Induces a Conformational Change in the TCF4::DNA Complex. *PLoS ONE*. https://doi.org/10.1371/journal.pone.0061867

Farbehi, N., Patrick, R., Dorison, A., Xaymardan, M., Janbandhu, V., Wystub-Lis, K., Ho, J. W. K., Nordon, R. E. and Harvey, R. P. (2019). Single-cell expression profiling reveals dynamic flux of cardiac stromal, vascular and immune cells in health and injury. *eLife* **8**, e43882. doi:10.7554/eLife.43882

Fiore, D., R.N. Judson, M. Low, S. Lee, E. Zhang, C. Hopkins, P. Xu, A. Lenzi, F.M. Rossi, and D.R. Lemos. 2016. Pharmacological blockage of fibro/adipogenic progenitor expansion and suppression of regenerative fibrogenesis is associated with impaired skeletal muscle regeneration. *Stem Cell Res*. 17:161-169.

Frietze, S., Wang, R., Yao, L., Tak, Y., Ye, Z., Gaddis, M., Witt, H., Farnham, P., and Jin, V., 2012. Cell type-specific binding patterns reveal that TCF7L2 can be tethered to the genome by association with GATA3. *Genome Biology* 13, R52.

Fu, X., Khalil, H., Kanisicak, O., Boyer, J. G., Vagnozzi, R. J., Maliken, B. D., … Molkentin, J. D. (2018). Specialized fibroblast differentiated states underlie scar formation in the infarcted mouse heart. *The Journal of Clinical Investigation*, 128(5), 2127–2143. https://doi.org/10.1172/JCI98215

Furtado, M. B., Nim, H. T., Boyd, S. E. and Rosenthal, N. A. (2016). View from the heart: cardiac fibroblasts in development, scarring and regeneration. *Development* 143, 387-397. doi:10.1242/dev.120576

Girardi, F., & Le Grand, F. (2018). Chapter Five - Wnt Signaling in Skeletal Muscle Development and Regeneration. In J. Larraín & G. B. T.-P. in M. B. and T. S. Olivares (Eds.), WNT Signaling in Health and Disease (Vol. 153, pp. 157–179). Academic Press. https://doi.org/https://doi.org/10.1016/bs.pmbts.2017.11.026

Gonzalez, D., O. Contreras, D.L. Rebolledo, J.P. Espinoza, B. van Zundert, and E. Brandan. 2017. ALS skeletal muscle shows enhanced TGF-beta signaling, fibrosis and induction of fibro/adipogenic progenitor markers. *PLoS One*. 12: e0177649.

Gosselin, L. E., Williams, J. E., Deering, M., Brazeau, D., Koury, S., & Martinez, D. A. (2004). Localization and early time course of TGF-β1 mRNA expression in dystrophic muscle. Muscle and Nerve. https://doi.org/10.1002/mus.20150

Götze, S., Coersmeyer, M., Müller, O., & Sievers, S. (2014). Histone deacetylase inhibitors induce attenuation of Wnt signaling and TCF7L2 depletion in colorectal carcinoma cells. *International Journal of Oncology*, 45, 1715-1723. https://doi.org/10.3892/ijo.2014.2550

Grant, S. F. A., Thorleifsson, G., Reynisdottir, I., Benediktsson, R., Manolescu, A., Sainz, J., … Stefansson, K. (2006). Variant of transcription factor 7-like 2 (TCF7L2) gene confers risk of type 2 diabetes. *Nature Genetics*, 38, 320–323. https://doi.org/10.1038/ng1732

Greer, C. B., Tanaka, Y., Kim, Y. J., Xie, P., Zhang, M. Q., Park, I.-H., & Kim, T. H. (2015). Histone Deacetylases Positively Regulate Transcription through the Elongation Machinery. *Cell Reports*, 13(7), 1444–1455. https://doi.org/10.1016/j.celrep.2015.10.013

Gutierrez, J., C.A. Droppelmann, O. Contreras, C. Takahashi, and E. Brandan. 2015. RECK-Mediated beta1-Integrin Regulation by TGF-beta1 Is Critical for Wound Contraction in Mice. *PLoS One*. 10: e0135005.

Hamburg-Shields, E., DiNuoscio, G. J., Mullin, N. K., Lafyatis, R., & Atit, R. P. (2015). Sustained β-catenin activity in dermal fibroblasts promotes fibrosis by up-regulating expression of extracellular matrix protein-coding genes. The Journal of Pathology, 235(5), 686–697. https://doi.org/10.1002/path.4481

Hamilton, T.G., R.A. Klinghoffer, P.D. Corrin, and P. Soriano. 2003. Evolutionary divergence of platelet-derived growth factor alpha receptor signaling mechanisms. *Mol Cell Biol*. 23: 4013-4025.

He, W., Zhang, L., Ni, A., Zhang, Z., Mirotsou, M., Mao, L., … Dzau, V. J. (2010). Exogenously administered secreted frizzled related protein 2 (Sfrp2) reduces fibrosis and improves cardiac function in a rat model of myocardial infarction. *Proceedings of the National Academy of Sciences*, 107(49), 21110 LP – 21115. https://doi.org/10.1073/pnas.1004708107

He, W., Dai, C., Li, Y., Zeng, G., Monga, S. P., & Liu, Y. (2009). Wnt/β-Catenin Signaling Promotes Renal Interstitial Fibrosis. *Journal of the American Society of Nephrology,* 20(4), 765 LP – 776. https://doi.org/10.1681/ASN.2008060566

Henderson, W. R., Chi, E. Y., Ye, X., Nguyen, C., Tien, Y., Zhou, B., … Kahn, M. (2010). Inhibition of Wnt/β-catenin/CREB binding protein (CBP) signaling reverses pulmonary fibrosis. *Proceedings of the National Academy of Sciences*, 107(32), 14309 LP – 14314. https://doi.org/10.1073/pnas.1001520107

Heredia, J.E., L. Mukundan, F.M. Chen, A.A. Mueller, R.C. Deo, R.M. Locksley, T.A. Rando, and A. Chawla. 2013. Type 2 innate signals stimulate fibro/adipogenic progenitors to facilitate muscle regeneration. *Cell*. 153:376-388.

Hinz, B., S.H. Phan, V.J. Thannickal, A. Galli, M.L. Bochaton-Piallat, and G. Gabbiani. 2007. The myofibroblast: one function, multiple origins. *Am J Pathol*. 170:1807-1816.

Ishitani, T., Ninomiya-Tsuji, J., & Matsumoto, K. (2003). Regulation of Lymphoid Enhancer Factor 1/T-Cell Factor by Mitogen-Activated Protein Kinase-Related Nemo-Like Kinase-Dependent Phosphorylation in Wnt/β-Catenin Signaling. *Molecular and Cellular Biology*, 23(4), 1379 LP-1389. https://doi.org/10.1128/MCB.23.4.1379-1389.2003

Jin, T. (2016). Current Understanding on Role of the Wnt Signaling Pathway Effector TCF7L2 in Glucose Homeostasis. *Endocrine Reviews*, 37(3), 254–277. https://doi.org/10.1210/er.2015-1146

Joe, A.W., L. Yi, A. Natarajan, F. Le Grand, L. So, J. Wang, M.A. Rudnicki, and F.M. Rossi. 2010. Muscle injury activates resident fibro/adipogenic progenitors that facilitate myogenesis. *Nat Cell Biol*. 12:153-163.

Jones, D. L., Haak, A. J., Caporarello, N., Choi, K. M., Ye, Z., Yan, H., … Tschumperlin, D. J. (2019). TGFβ-induced fibroblast activation requires persistent and targeted HDAC-mediated gene repression. *Journal of Cell Science*, 132(20), jcs233486. https://doi.org/10.1242/jcs.233486

Judson, R. N., Low, M., Eisner, C., & Rossi, F. M. (2017). Isolation, Culture, and Differentiation of Fibro/Adipogenic Progenitors (FAPs) from Skeletal Muscle. In Methods in molecular biology (Clifton, N.J.). https://doi.org/10.1007/978-1-4939-7283-8_7

Kanisicak, O., Khalil, H., Ivey, M. J., Karch, J., Maliken, B. D., Correll, R. N., Brody, M. J., J. Lin, S.-C., Aronow, B. J., Tallquist, M. D. et al. (2016). Genetic lineage tracing defines myofibroblast origin and function in the injured heart. *Nat. Commun*. 7, 12260. doi:10.1038/ncomms12260

Kardon, G., Harfe, B. D., & Tabin, C. J. (2003). A Tcf4-Positive Mesodermal Population Provides a Prepattern for Vertebrate Limb Muscle Patterning. *Developmental Cell*, 5(6), 937–944. https://doi.org/10.1016/S1534-5807(03)00360-5

Kim, K.K., D. Sheppard, and H.A. Chapman. 2018. TGF-beta1 Signaling and Tissue Fibrosis. *Cold Spring Harb Perspect Biol*. 10.

Konigsho, M. et al. Functional Wnt signaling is increased in idiopathic pulmonary fibrosis. *PLoS One*. 3, e2142 (2008).

Kopinke, D., E.C. Roberson, and J.F. Reiter. 2017. Ciliary Hedgehog Signaling Restricts Injury-Induced Adipogenesis. *Cell*. 170:340-351 e312.

Korinek V, Barker N, Moerer P & van Donselaar E., 1998. Depletion of epithelial stem-cell compartments in the small intestine of mice lacking Tcf-4. *Nature genetics*. 18, 379-383.

Korinek, V, Barker, N., Morin, P.J., van Wichen, D., de Weger, R., Kinzler, K.W., Vogelstein, B., and Clevers, H., 1997. Constitutive Transcriptional Activation by a beta-catenin-Tcf complex in APC -/- Colon Carcinoma. *Science*, 275: 1784-1787

Lemos, D.R., F. Babaeijandaghi, M. Low, C.K. Chang, S.T. Lee, D. Fiore, R.H. Zhang, A. Natarajan, S.A. Nedospasov, and F.M. Rossi. 2015. Nilotinib reduces muscle fibrosis in chronic muscle injury by promoting TNF-mediated apoptosis of fibro/adipogenic progenitors. *Nat Med*. 21:786-794.

Lemos, D. R. and Duffield, J. S. (2018). Tissue-resident mesenchymal stromal cells: Implications for tissue-specific antifibrotic therapies. *Science Translational Medicine*. doi:10.1126/scitranslmed.aan5174

Lepper, C., T.A. Partridge, and C.M. Fan. 2011. An absolute requirement for Pax7-positive satellite cells in acute injury-induced skeletal muscle regeneration. *Development*. 138:3639-3646.

Lien WH, Fuchs E., 2014. Wnt some lose some: transcriptional governance of stem cells by Wnt/beta-catenin signaling. *Genes Dev*. 28:1517–1532.

Lien, W. H., Polak, L., Lin, M., Lay, K., Zheng, D., & Fuchs, E. (2014). In vivo transcriptional governance of hair follicle stem cells by canonical Wnt regulators. *Nature Cell Biology*. https://doi.org/10.1038/ncb2903

Liu, L. et al. Wnt pathway in pulmonary fibrosis in the bleomycin mouse model. *J. Environ. Pathol. Toxicol*. Oncol. 28, 99–108 (2009).

Lukjanenko, L., Karaz, S., Stuelsatz, P., Rudnicki, M. A., Bentzinger, C. F., Feige, J. N., … Michaud, J. (2019). Aging Disrupts Muscle Stem Cell Function by Impairing Matricellular WISP1 Secretion from Fibro-Adipogenic Progenitors Stem Cell, 1–14. https://doi.org/10.1016/j.stem.2018.12.014

Lynch, M. D. and Watt, F. M. (2018). Fibroblast heterogeneity: implications for human disease. *J. Clin. Investig*. 128, 26-35. doi:10.1172/JCI93555

Mackey, A.L., M. Magnan, B. Chazaud, and M. Kjaer. 2017. Human skeletal muscle fibroblasts stimulate in vitro myogenesis and in vivo muscle regeneration. *J Physiol*. 595:5115-5127.

Malecova, B., S. Gatto, U. Etxaniz, M. Passafaro, A. Cortez, C. Nicoletti, L. Giordani, A. Torcinaro, M. De Bardi, S. Bicciato, F. De Santa, L. Madaro, and P.L. Puri. 2018. Dynamics of cellular states of fibro-adipogenic progenitors during myogenesis and muscular dystrophy. *Nat Commun*. 9:3670.

Mahmoudi, S., Mancini, E., Xu, L., Moore, A., Jahanbani, F., Hebestreit, K., … Brunet, A. (2019). Heterogeneity in old fibroblasts is linked to variability in reprogramming and wound healing. *Nature*, 574(7779), 553–558. https://doi.org/10.1038/s41586-019-1658-5

Mann, C.J., E. Perdiguero, Y. Kharraz, S. Aguilar, P. Pessina, A.L. Serrano, and P. Munoz-Canoves. 2011. Aberrant repair and fibrosis development in skeletal muscle. *Skelet Muscle*. 1:21.

Masur, S., & Dewal, H. (1996). Myofibroblasts differentiate from fibroblasts when plated at low density. Proceedings of the National Academy of Sciences of the United States of America. https://doi.org/10.1073/pnas.93.9.4219

Massagué, J., Cheifetz, S., Endo, T., & Nadal-Ginard, B. (1986). Type beta transforming growth factor is an inhibitor of myogenic differentiation. Proceedings of the National Academy of Sciences, 83(21), 8206 LP-8210. https://doi.org/10.1073/pnas.83.21.8206

Massagué, J. (1998). TGF-beta signal transduction. *Annu Rev Biochem*. https://doi.org/10.1146/annurev.biochem.67.1.753

Massagué, J. (2012). TGFβ signalling in context. *Nature Reviews Molecular Cell Biology*. https://doi.org/10.1038/nrm3434

Mathew, S.J., J.M. Hansen, A.J. Merrell, M.M. Murphy, J.A. Lawson, D.A. Hutcheson, M.S. Hansen, M. Angus-Hill, and G. Kardon. 2011. Connective tissue fibroblasts and Tcf4 regulate myogenesis. *Development*. 138: 371-384.

McBeath, R., Pirone, D. M., Nelson, C. M., Bhadriraju, K., & Chen, C. S. (2004). Cell shape, cytoskeletal tension, and RhoA regulate stem cell lineage commitment. Developmental *Cell*. https://doi.org/10.1016/S1534-5807(04)00075-9

Merrell, A. J., Ellis, B. J., Fox, Z. D., Lawson, J. A., Weiss, J. A., & Kardon, G. (2015). Muscle connective tissue controls development of the diaphragm and is a source of congenital diaphragmatic hernias. *Nature Genetics*. https://doi.org/10.1038/ng.3250

Murphy, M.M., J.A. Lawson, S.J. Mathew, D.A. Hutcheson, and G. Kardon. 2011. Satellite cells, connective tissue fibroblasts and their interactions are crucial for muscle regeneration. *Development*. 138:3625-3637.

Nalepa, G., Rolfe, M., & Harper, J. W. (2006). Drug discovery in the ubiquitin-proteasome system. *Nature Reviews Drug Discovery*. https://doi.org/10.1038/nrd2056

Nusse, R., & Clevers, H. (2017). Wnt/β-Catenin Signaling, Disease, and Emerging Therapeutic Modalities. *Cell.* https://doi.org/10.1016/j.cell.2017.05.016

Oishi, T., Uezumi, A., Kanaji, A., Yamamoto, N., Yamaguchi, A., Yamada, H., et al. (2013). Osteogenic differentiation capacity of human skeletal muscle-derived progenitor cells. *PLoS ONE* 8:e56641. doi: 10.1371/journal.pone.0056641

Oliva, C. A., Montecinos-Oliva, C., & Inestrosa, N. C. (2018). Chapter Three - Wnt Signaling in the Central Nervous System: New Insights in Health and Disease. In J. Larraín & G. B. T.-P. in M. B. and T. S. Olivares

(Eds.), WNT Signaling in Health and Disease (Vol. 153, pp. 81–130). Academic Press. https://doi.org/https://doi.org/10.1016/bs.pmbts.2017.11.018

Pessina, P., Y. Kharraz, M. Jardi, S. Fukada, A.L. Serrano, E. Perdiguero, and P. Munoz-Canoves. 2015. Fibrogenic Cell Plasticity Blunts Tissue Regeneration and Aggravates Muscular Dystrophy. *Stem Cell Reports*. 4:1046-1060.

Petrilli, L. L., Spada, F., Fuoco, C., Micarelli, E., Reggio, A., Rosina, M., … Cesareni, G. (2017). Single-cell quantitative analysis of skeletal muscle cell population dynamics during regeneration and ageing. *BioRxiv*, 222158. https://doi.org/10.1101/222158

Piersma, B., Bank, R. A., & Boersema, M. (2015). Signaling in Fibrosis: TGF-β, WNT, and YAP/TAZ Converge. *Frontiers in Medicine*. https://doi.org/10.3389/fmed.2015.00059

Plikus, M. V., Guerrero-Juarez, C. F., Ito, M., Li, Y. R., Dedhia, P. H., Zheng, Y., Shao, M., Gay, D. L., Ramos, R., Hsi, T.-C. et al. (2017). Regeneration of fat cells from myofibroblasts during wound healing. *Science* 355, 748-752. doi:10.1126/science.aai8792

Ravindranath A, O'Connell A, Johnston PG, El-Tanani MK., 2008. The role of LEF/ TCF factors in neoplastic transformation. *Curr. Mol. Med*. 8, 38-50.

Reznikoff, C.A., J.S. Bertram, D.W. Brankow, and C. Heidelberger. 1973. Quantitative and qualitative studies of chemical transformation of cloned C3H mouse embryo cells sensitive to post-confluence inhibition of cell division. *Cancer Res*. 33:3239-3249.

Rinkevich, Y.,Walmsley, G. G., Hu, M. S., Maan, Z. N., Newman, A. M., Drukker, M., Januszyk, M., Krampitz, G. W., Gurtner, G. C., Lorenz, H. P. et al. (2015). Identification and isolation of a dermal lineage with intrinsic fibrogenic potential. *Science* 348, aaa2151. doi:10.1126/science.aaa2151

Riquelme, C., Larraín, J., Schönherr, E., Henriquez, J. P., Kresse, H., & Brandan, E. (2001). Antisense Inhibition of Decorin Expression in Myoblasts Decreases Cell Responsiveness to Transforming Growth Factor α and Accelerates Skeletal Muscle Differentiation. Journal of Biological Chemistry. https://doi.org/10.1074/jbc.M004602200

Riquelme-Guzmán, C., O. Contreras, and E. Brandan. 2018. Expression of CTGF/CCN2 in response to LPA is stimulated by fibrotic extracellular matrix via the integrin/FAK axis. *Am J Physiol Cell Physiol*. 314:C415-C427.

Rognoni, E., Pisco, A. O., Hiratsuka, T., Sipila , K. H., Belmonte, J. M., Mobasseri, S. A., Philippeos, C., Dilão, R. and Watt, F. M. (2018). Fibroblast state switching orchestrates dermal maturation and wound healing. *Mol. Syst. Biol*. 14, e8174. doi:10.15252/msb.20178174

Sambasivan, R., R. Yao, A. Kissenpfennig, L. Van Wittenberghe, A. Paldi, B. Gayraud-Morel, H. Guenou, B. Malissen, S. Tajbakhsh, and A. Galy. 2011. Pax7-expressing satellite cells are indispensable for adult skeletal muscle regeneration. *Development*. 138:3647-3656.

Schabort, E. J., van der Merwe, M., Loos, B., Moore, F. P., & Niesler, C. U. (2009). TGF-β's delay skeletal muscle progenitor cell differentiation in an isoform-independent manner. *Experimental Cell Research*, 315(3), 373–384. https://doi.org/https://doi.org/10.1016/j.yexcr.2008.10.037

Schuijers, J., Mokry, M., Hatzis, P., Cuppen, E., and Clevers, H., 2014. Wnt-induced transcriptional activation is exclusively mediated by TCF/LEF. *EMBO J*, 33, 146–156.

Seo, H.-H., Lee, S., Lee, C. Y., Lee, J., Shin, S., Song, B.-W., … Hwang, K.-C. (2019). Multipoint targeting of TGF-β/Wnt transactivation circuit with microRNA 384-5p for cardiac fibrosis. *Cell Death & Differentiation*, 26(6), 1107–1123. https://doi.org/10.1038/s41418-018-0187-3

Seto, E., & Yoshida, M. (2014). Erasers of Histone Acetylation: The Histone Deacetylase Enzymes. *Cold Spring Harbor Perspectives in Biology*, 6(4). https://doi.org/10.1101/cshperspect.a018713

Shy, B. R., Wu, C. I., Khramtsova, G. F., Zhang, J. Y., Olopade, O. I., Goss, K. H., & Merrill, B. J. (2013). Regulation of Tcf7l1 DNA Binding and Protein Stability as Principal Mechanisms of Wnt/β-Catenin Signaling. *Cell Reports*. https://doi.org/10.1016/j.celrep.2013.06.001

Singh, R., J.N. Artaza, W.E. Taylor, N.F. Gonzalez-Cadavid, and S. Bhasin. 2003. Androgens stimulate myogenic differentiation and inhibit adipogenesis in C3H/10T1/2 pluripotent cells through an androgen receptor-mediated pathway. *Endocrinology*. 144:5081-5088.

Smith, L. R. and Barton, E. R. (2018). Regulation of fibrosis in muscular dystrophy. *Matrix Biol*. 68-69, 602-615. doi:10.1016/j.matbio.2018.01.014

Song, Y., Lee, S., Kim, J.R., Jho, E-H. (2018). Pja2 Inhibits Wnt/β-catenin Signaling by Reducing the Level of TCF/LEF1. *International Journal of Stem Cells*, 11(2), 242–247. https://doi.org/10.15283/ijsc18032

Soliman, H., Paylor, B., Scott, W., Lemos, D., Chang, C., Arostegui, M., … Rossi, F. (2019). Pathogenic potential of Hic1 expressing cardiac stromal progenitors. *BioRxiv*, 544403. https://doi.org/10.1101/544403

Stark, C. (2006). BioGRID: a general repository for interaction datasets. *Nucleic Acids Research*. https://doi.org/10.1093/nar/gkj109

Surendran, K., McCaul, S. P. & Simon, T. C. A role for Wnt-4 in renal fibrosis. *Am. J. Physiol. Renal. Physiol*. 282, F431–F441 (2002).

Suzuki, K., Bose, P., Leong-Quong, R. Y., Fujita, D. J., & Riabowol, K. (2010). REAP: A two minute cell fractionation method. *BMC Research Notes*. https://doi.org/10.1186/1756-0500-3-294

Tang, W., Dodge, M., Gundapaneni, D., Michnoff, C., Roth, M., & Lum, L. (2008). A genome-wide RNAi screen for Wnt/β-catenin pathway components identifies unexpected roles for TCF transcription factors in cancer. *Proceedings of the National Academy of Sciences*, 105(28), 9697 LP – 9702. https://doi.org/10.1073/pnas.0804709105

Tan, S. H., & Barker, N. (2018). Chapter Two - Wnt Signaling in Adult Epithelial Stem Cells and Cancer. In J. Larraín & G. B. T.-P. in M. B. and T. S. Olivares (Eds.), WNT Signaling in Health and Disease (Vol. 153, pp. 21–79). *Academic Press*. https://doi.org/https://doi.org/10.1016/bs.pmbts.2017.11.017

Tallquist, M. D., & Molkentin, J. D. (2017). Redefining the identity of cardiac fibroblasts. *Nature Reviews Cardiology*. https://doi.org/10.1038/nrcardio.2017.57

The Tabula Muris Consortium, Overall coordination, Logistical coordination, Organ collection and processing; Library preparation and sequencing, Computational data analysis, Cell type annotation, Writing group, Supplemental text writing group and Principal investigators. (2018). Single-cell transcriptomics of 20 mouse organs creates a Tabula Muris. *Nature* **562**, 367-372. doi:10.1038/s41586-018-0590-4

Trensz, F., Haroun, S., Cloutier, A., Richter, M. V. & Grenier, G. A muscle resident cell population promotes fibrosis in hindlimb skeletal muscles of mdx mice through the Wnt canonical pathway. *Am. J. Physiol. Cell Physiol*. 299, C939–C947 (2010).

Uezumi, A., S. Fukada, N. Yamamoto, M. Ikemoto-Uezumi, M. Nakatani, M. Morita, A. Yamaguchi, H. Yamada, I. Nishino, Y. Hamada, and K. Tsuchida. 2014a. Identification and characterization of PDGFRalpha+ mesenchymal progenitors in human skeletal muscle. *Cell Death Dis*. 5: e1186.

Uezumi, A., M. Ikemoto-Uezumi, and K. Tsuchida. 2014b. Roles of nonmyogenic mesenchymal progenitors in pathogenesis and regeneration of skeletal muscle. *Front Physiol*. 5:68.

Uezumi, A., S. Fukada, N. Yamamoto, S. Takeda, and K. Tsuchida. 2010. Mesenchymal progenitors distinct from satellite cells contribute to ectopic fat cell formation in skeletal muscle. *Nat Cell Biol*. 12:143-152.

Uezumi, A., T. Ito, D. Morikawa, N. Shimizu, T. Yoneda, M. Segawa, M. Yamaguchi, R. Ogawa, M.M. Matev, Y. Miyagoe-Suzuki, S. Takeda, K. Tsujikawa, K. Tsuchida, H. Yamamoto, and S. Fukada. 2011. Fibrosis and adipogenesis originate from a common mesenchymal progenitor in skeletal muscle. *Journal of Cell Science*. 124:3654-3664.

Vallecillo-García, P., M. Orgeur, S. Vom Hofe-Schneider, J. Stumm, V. Kappert, D.M. Ibrahim, S.T. Borno, S. Hayashi, F. Relaix, K. Hildebrandt, G. Sengle, M. Koch, B. Timmermann, G. Marazzi, D.A. Sassoon, D. Duprez, and S. Stricker. 2017. Odd skipped-related 1 identifies a population of embryonic fibro-adipogenic progenitors regulating myogenesis during limb development. *Nat Commun*. 8:1218.

van de Wetering, M., Oosterwegel, M., Dooijes, D., and Clevers, H.C., 1991. Identification and cloning of TCF-1, a T cell-specific transcription factor containing a sequence-specific HMG box. *EMBO J.*, 10, 123-132

van de Wetering, M., Sancho, E., Verweij, C., de Lau, W., Oving, I., Hurlstone, A., Van der Horn, K., Batlle, E., Coudreuse, D., Haramis, A-P., Tjon-Pon-Fong, M., Moerer, P., Van den Born, M., Soete, G., Pals, S., Eilers, M., Medema, R., Clevers, H., 2002. The beta-catenin/TCF4 complex imposes a crypt progenitor phenotype on colorectal cancer cells. *Cell*, 111, 241-250

Vallée, A., Lecarpentier, Y., Guillevin, R., & Vallée, J.-N. (2017). Interactions between TGF-β, canonical WNT/β-catenin pathway and PPARγ in radiation-induced fibrosis. *Oncotarget*; Vol 8, No 52. Retrieved from http://legacy.oncotarget.com/index.php?journal=oncotarget&amp

Vidal, B., Serrano, A. L., Tjwa, M., Suelves, M., Ardite, E., De Mori, R., … Muñoz-Cánoves, P. (2008). Fibrinogen drives dystrophic muscle fibrosis via a TGFβ/alternative macrophage activation pathway. *Genes and Development*. https://doi.org/10.1101/gad.465908

Wei, J. et al. Canonical Wnt signaling induces skin fibrosis and subcutaneous lipoatrophy: a novel mouse model for scleroderma? *Arthritis Rheum*. 63, 1707–1717 (2011).

Weise, A., Bruser, K., Elfert, S., Wallmen, B., Wittel, Y., Wohrle, S. and Hecht, A. (2010) Alternative splicing of Tcf7l2 transcripts generates protein variants with differential promoter-binding and transcriptional activation properties at Wnt/beta-catenin targets. *Nucleic Acids Res.*, 38, 1964–1981.

Wosczyna, M.N., A.A. Biswas, C.A. Cogswell, and D.J. Goldhamer. 2012. Multipotent progenitors resident in the skeletal muscle interstitium exhibit robust BMP-dependent osteogenic activity and mediate heterotopic ossification. *J Bone Miner Res*. 27:1004-1017.

Wosczyna, M.N., and T.A. Rando. 2018. A Muscle Stem Cell Support Group: Coordinated Cellular Responses in Muscle Regeneration. *Dev Cell*. 46:135-143.

Wosczyna, M. N., Konishi, C. T., Perez Carbajal, E. E.,Wang, T. T.,Walsh, R. A., Gan, Q.,Wagner, M.W. and Rando, T. A. (2019). Mesenchymal stromal cells are required for regeneration and homeostatic maintenance of skeletal muscle. *Cell Rep*. 27, 2029-2035.e5. doi:10.1016/j.celrep.2019.04.074

Wynn, T. A., & Ramalingam, T. R. (2012). Mechanisms of fibrosis: Therapeutic translation for fibrotic disease. *Nature Medicine*. https://doi.org/10.1038/nm.2807

Xiang, F. L., Fang, M., & Yutzey, K. E. (2017). Loss of β-catenin in resident cardiac fibroblasts attenuates fibrosis induced by pressure overload in mice. *Nature Communications*. https://doi.org/10.1038/s41467-017-00840-w

Yamada, M., Ohnishi, J., Ohkawara, B., Iemura, S., Satoh, K., Hyodo-Miura, J., … Shibuya, H. (2006). NARF, an Nemo-like Kinase (NLK)-associated Ring Finger Protein Regulates the Ubiquitylation and Degradation of T Cell Factor/Lymphoid Enhancer Factor (TCF/LEF). *Journal of Biological Chemistry* , 281(30), 20749–20760. https://doi.org/10.1074/jbc.M602089200

Yamamoto, H., Ihara, M., Matsuura, Y., & Kikuchi, A. (2003). Sumoylation is involved in β-catenin-dependent activation of Tcf-4. *EMBO Journal*. https://doi.org/10.1093/emboj/cdg204

Yuan, T., Yan, F., Ying, M., Cao, J., He, Q., Zhu, H., & Yang, B. (2018). Inhibition of Ubiquitin-Specific Proteases as a Novel Anticancer Therapeutic Strategy. *Frontiers in Pharmacology*. https://doi.org/10.3389/fphar.2018.01080. Retrieved from https://www.frontiersin.org/article/10.3389/fphar.2018.01080

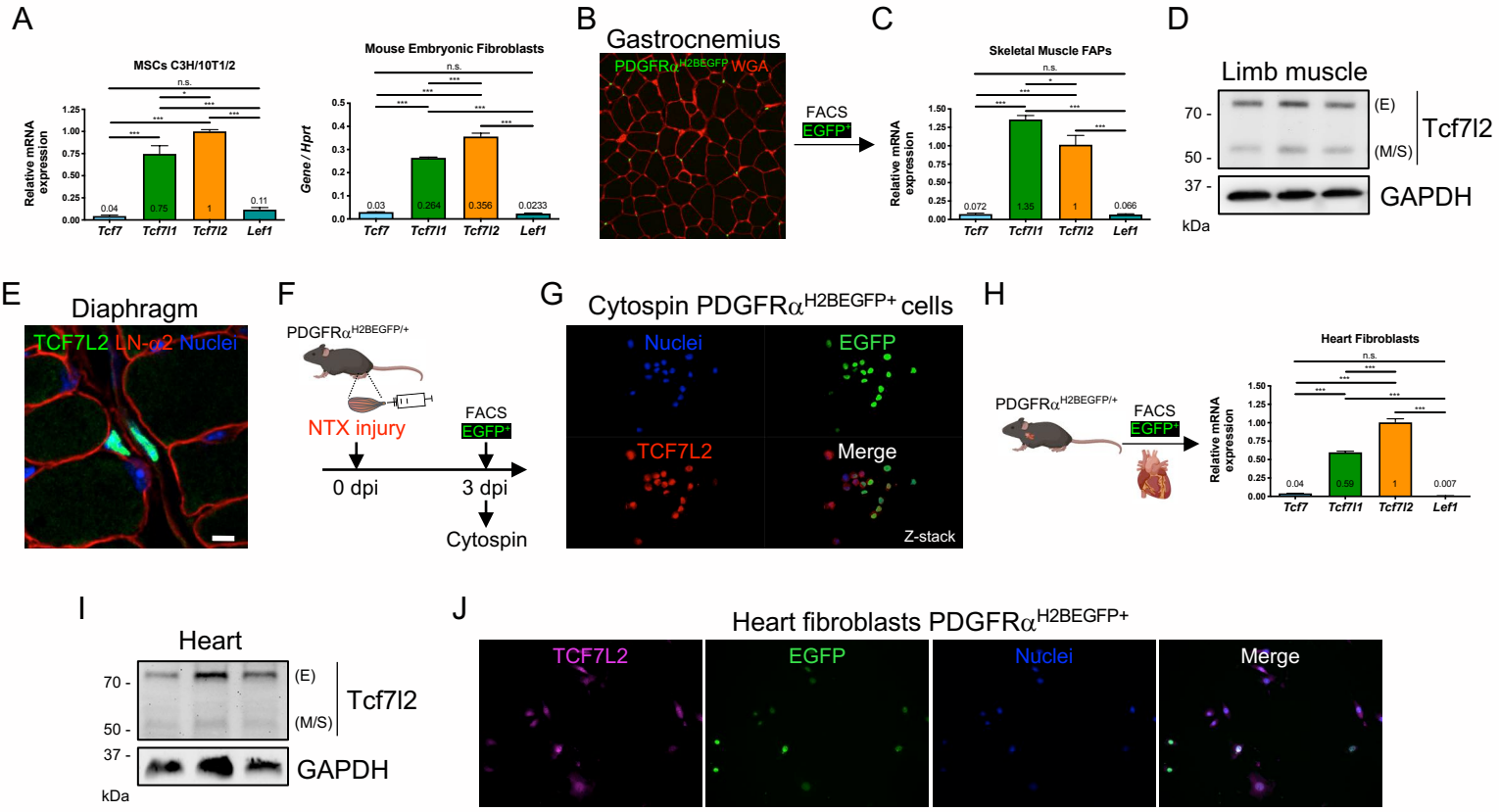

Fig. 1. Differential expression of Tcf/Lef transcription factors in mesenchymal stromal cells and fibroblasts.

(A) *Tcf7*, *Tcf7l1*, *Tcf7l2*, and *Lef1* mRNA expression levels were analyzed by quantitative PCR in C3H/10T1/2 mesenchymal progenitors and MEFs at growing conditions. ***P<0.001; *P<0.05; n.s., not significant by one-way ANOVA with Dunnett's post-test; n=4. (B) Skeletal muscle FAPs were FACS-isolated from the PDGFRα^{H2BEGFP} reporter mice. WGA staining labels ECM. (C) *Tcf7*, *Tcf7l1*, *Tcf7l2*, and *Lef1* mRNA expression levels were analyzed by quantitative PCR in EGFP$^+$ FAPs at growing conditions. ***P<0.001; *P<0.05; n.s., not significant by one-way ANOVA with Dunnett's post-test; n=3. (D) Representative western blot analysis showing TCF7L2 protein levels in gastrocnemius skeletal muscle. GAPDH was used as the loading control. (E) Confocal image of TCF7L2 immunofluorescence, showing its nuclei-specific subcellular localization in stromal cells. Laminin-α2 (LN-α2) (*red*) and nuclei (Hoechst in *blue*) were also stained. Scale bar: 10 μm. (F) Strategy used to isolate transit amplifying EGFP$^+$ FAPs at day 3 post NTX TA injury. (G) Z-stack confocal image from cytospined EGFP$^+$ FAPs showing TCF7L2 nuclear expression in PDGFRα-EGFP$^+$ stromal cells. (H) *Tcf7*, *Tcf7l1*, *Tcf7l2*, and *Lef1* mRNA expression levels were analyzed by quantitative PCR in cardiac fibroblasts at growing conditions. ***P<0.001; n.s., not significant by one-way ANOVA with Dunnett's post-test; n=3. (I) Representative western blot analysis showing TCF7L2 protein levels in whole heart tissue. GAPDH was used as the loading control. (J) Immunofluorescence of TCF7L2 (*magenta*) in isolated heart PDGFRα-EGFP$^+$ stromal cells in growing conditions.

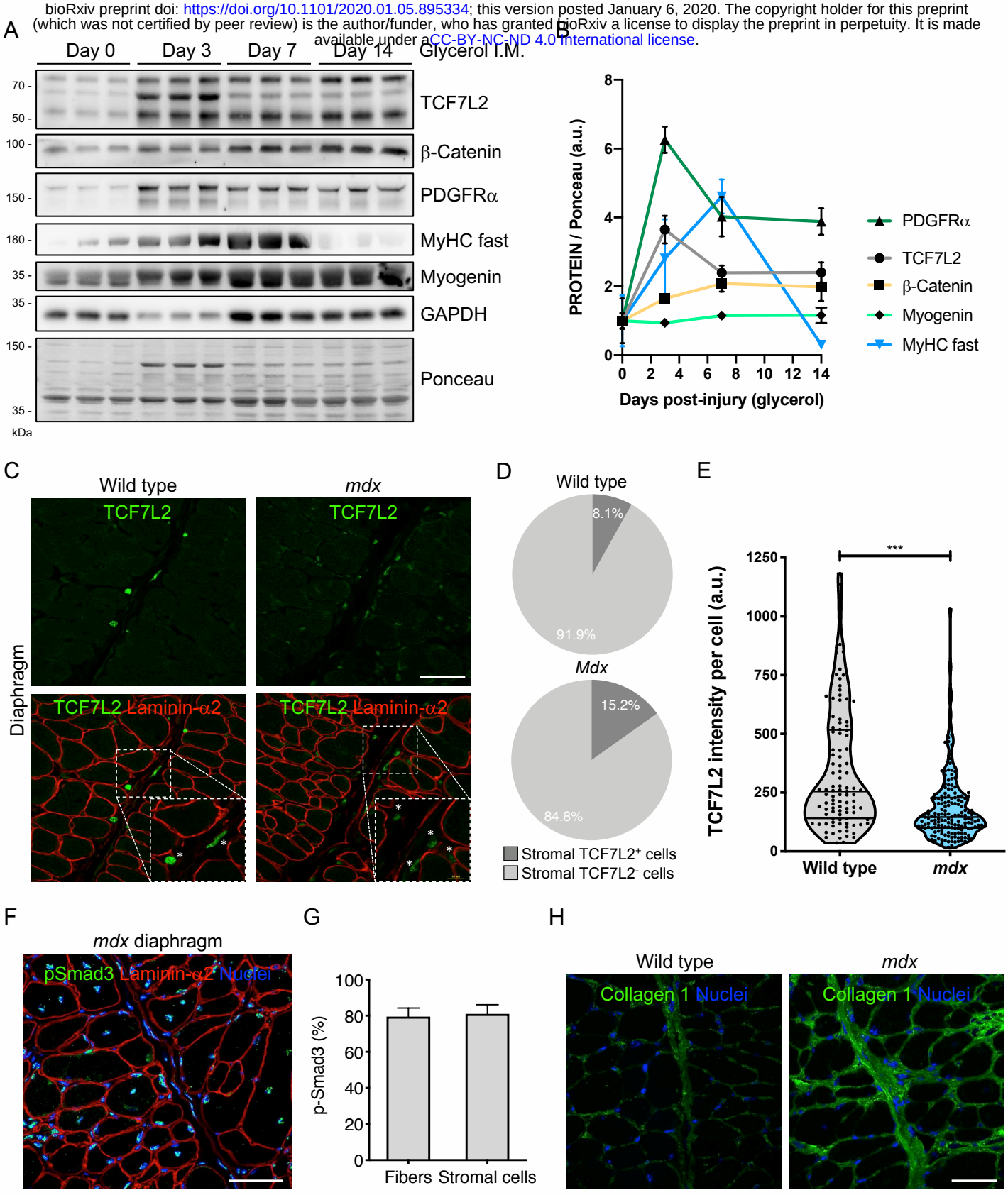

Fig. 2. Dynamics of TCF7L2 expression in the stromal compartment during regeneration and repair.

(A) Representative western blot analysis showing TCF7L2, B-Catenin, PDGFRα, MyHC fast, Myogenin, and GAPDH in TA skeletal musce mesenchymal progenitor cells after damage with glycerol at different time points (0, 3, 7 and 14 day). Ponceau red was used as the loading control. (B) Quantification of TCF7L2, β-Catenin, PDGFRα, MyHC fast, and Myogenin protein expression. *n*=3. (C) Z-stack confocal images showing the localization of TCF7L2$^+$ cells in diaphragm muscle sections of adult wild-type and from the dystrophic *mdx* mice. Scale bars: 50 μm and 10 μm. (D) Quantification of the fluorescence intensity of TCF7L2 in stromal TCF7L2$^+$ cells. ***P<0.001; by two-tailed Student's t-test. *n*=4. (F) Representative confocal image showing the localization of phosphorylated Smad3$^+$ cells in diaphragm muscle sections of adult *mdx* mice. Scale bar: 50 μm. (G) Quantification of the percentage of p-Smad3$^+$ cells. *n*=4. (H) Representative confocal image showing the increase of ECM collagen type 1 immunostaining in diaphragm of *mdx* when compared to wild-type mice.

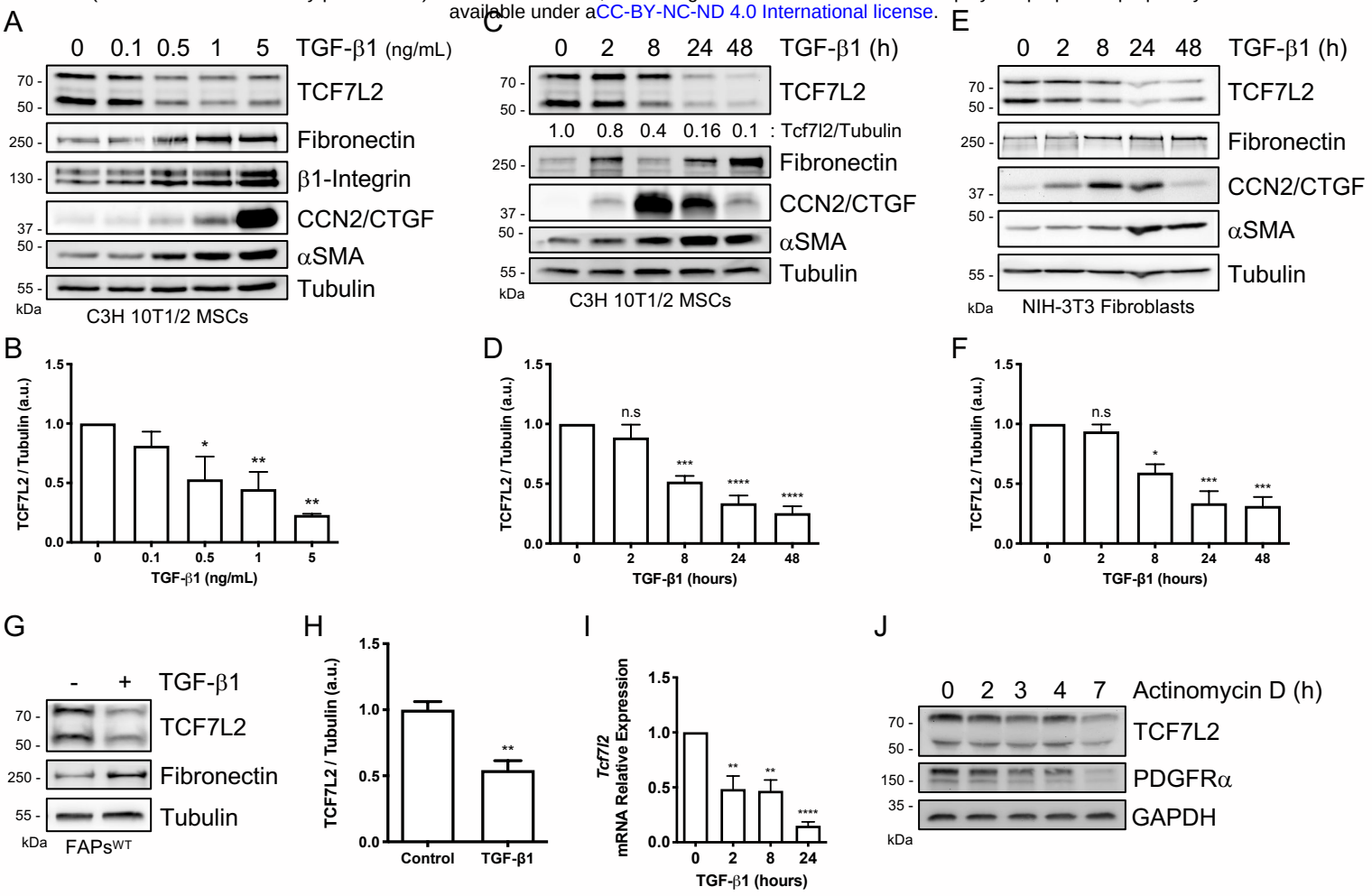

Fig. 3. TGF-β signaling downregulates the expression of TCF7L2 in FAPs and mesenchymal progenitor cells.

(A) Representative western blot analysis showing TCF7L2, fibronectin, β1-Integrin, CCN2/CTGF, and αSMA expression levels in C3H/10T1/2 MSCs after treatment with different concentrations of TGF-β1 for 24 h. Tubulin was used as the loading control. (B) Quantification of TCF7L2 protein expression. ***P*<0.005; **P*<0.05 by one-way ANOVA with Dunnett's post-test; *n*=4. (C,E) Representative western blot analysis showing TCF7L2, fibronectin, CCN2/CTGF, and αSMA expression levels in (C) C3H/10T1/2 mesenchymal progenitor cells and (E) NIH-3T3 fibroblasts after treatment with TGF-β1 (5 ng/ml) at different time points (0, 2, 8, 24, 48 h). Tubulin was used as the loading control. (D,F) Quantification of TCF7L2 protein expression. *****P*<0.0001; ****P*<0.001; **P*<0.05; n.s., not significant by one-way ANOVA with Dunnett's post-test; *n*=4. (G) Representative western blot analysis showing TCF7L2 and fibronectin expression levels after treatment with 5 ng/ml TGF-β1 (24 h) in PDGFRα-EGFP^{+} FAPs. Tubulin was used as the loading control. (H) Quantification of TCF7L2 protein expression. ***P*<0.005 by two-tailed Student's t-test; *n*=3. (I) *Tcf7l2* mRNA expression levels were analyzed by quantitative PCR in C3H/10T1/2 mesenchymal progenitors after 2, 8 and 24 h of treatment with TGF-β1 (5 ng/ml). ****P<0.0001; **P<0.005 by one-way ANOVA with Dunnett's post-test; *n*=3. (J) Representative western blot analysis showing TCF7L2 and PDGFRα expression levels after treatment with actinomycin D at different time points (0, 2, 3, 4, 7 h). GAPDH was used as the loading control.

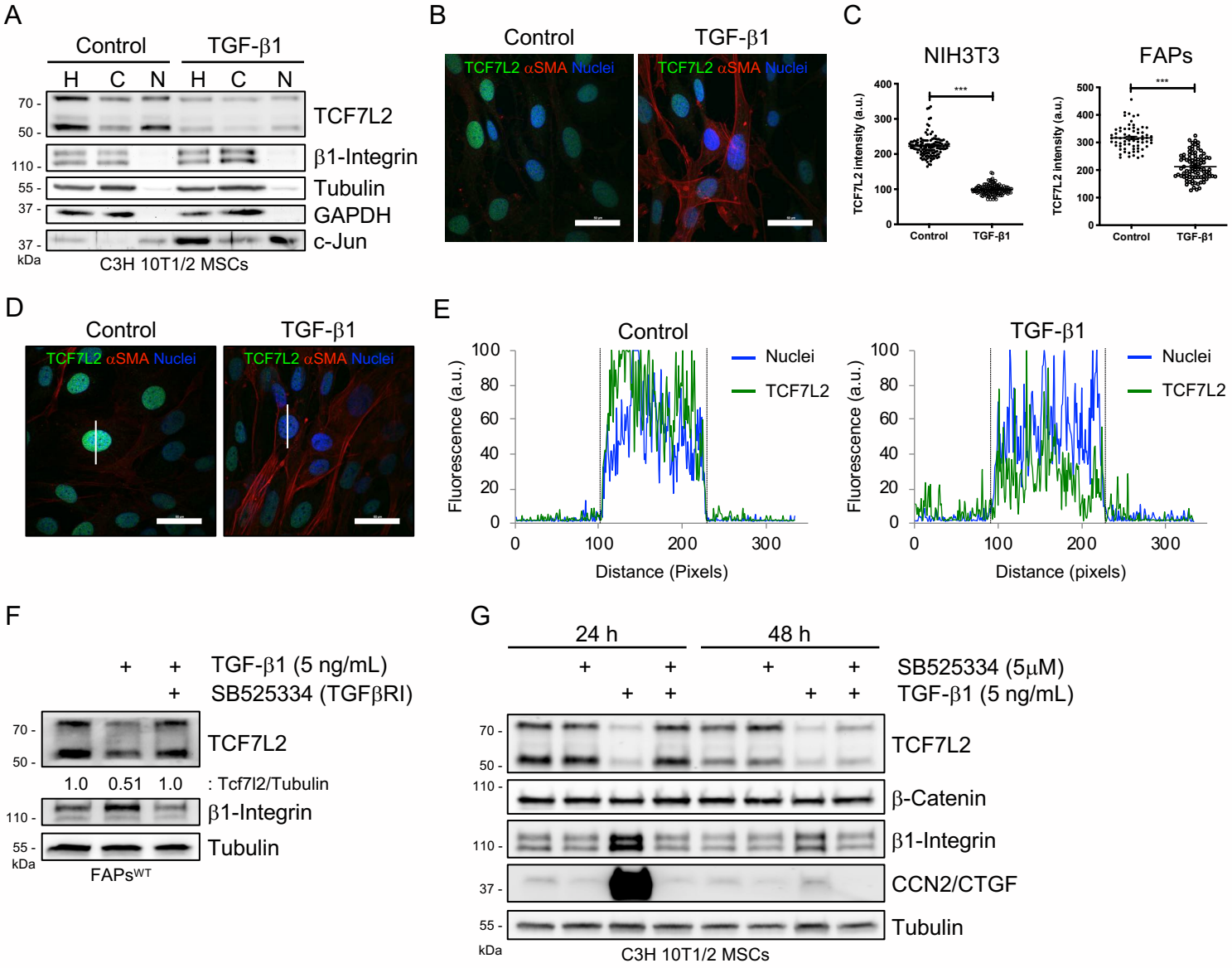

Fig. 4. Extracellular TGF-β reduces the expression of TCF7L2 through TGFβR1.

(A) Representative western blot analysis showing TCF7L2, β1-Integrin, tubulin, GAPDH, and c-Jun expression levels in control and TGF-β1-treated C3H/10T1/2 cells. H: Whole cell lysate; C: Cytoplasmic lysate; N: Nuclei lysate. (B) Z-stack confocal images showing localization of TCF7L2 (*green*) and αSMA (*red*) in control and TGF-β1-treated (36 h) C3H/10T1/2 MSCs. Scale bars: 50 μm. (C) Quantification of the TCF7L2 fluorescence intensity in NIH-3T3 and FAPs. (a.u.: arbitrary units). Each dot represents a single cell quantified were a ROI area was previously defined. ***P<0.001; by two-tailed Student's t-test. n=3. (D) Z-stack confocal images showing localization of TCF7L2 (*green*) and αSMA (*red*) in control and TGF-β1-treated (24 h) C3H/10T1/2 MSCs. Scale bars: 50 μm. (E) Label-distribution graph showing the fluorescence intensity of TCF7L2 and Hoechst along the cell axis as shown in (D) with the *white* line. Distance is shown in pixels. Dotted lines show the nucleus-cytoplasm boundary. (a.u.: arbitrary units). (F) Representative western blot analysis showing TCF7L2 and β1-Integrin expression levels in wild-type FAPs co-treated for 24 h with TGFBR1 inhibitor SB525334 (5 μM) and TGF-β1 (5 ng/ml). Tubulin was used as the loading control. (G) Representative western blot analysis showing TCF7L2, β-Catenin, β1-Integrin, and CCN2/CTGF expression levels in C3H/10T1/2 MSCs co-treated for 24 h or 48 h with TGFBR1 inhibitor SB525334 (5 μM) and TGF-β1 (5 ng/ml). Tubulin was used as the loading control.

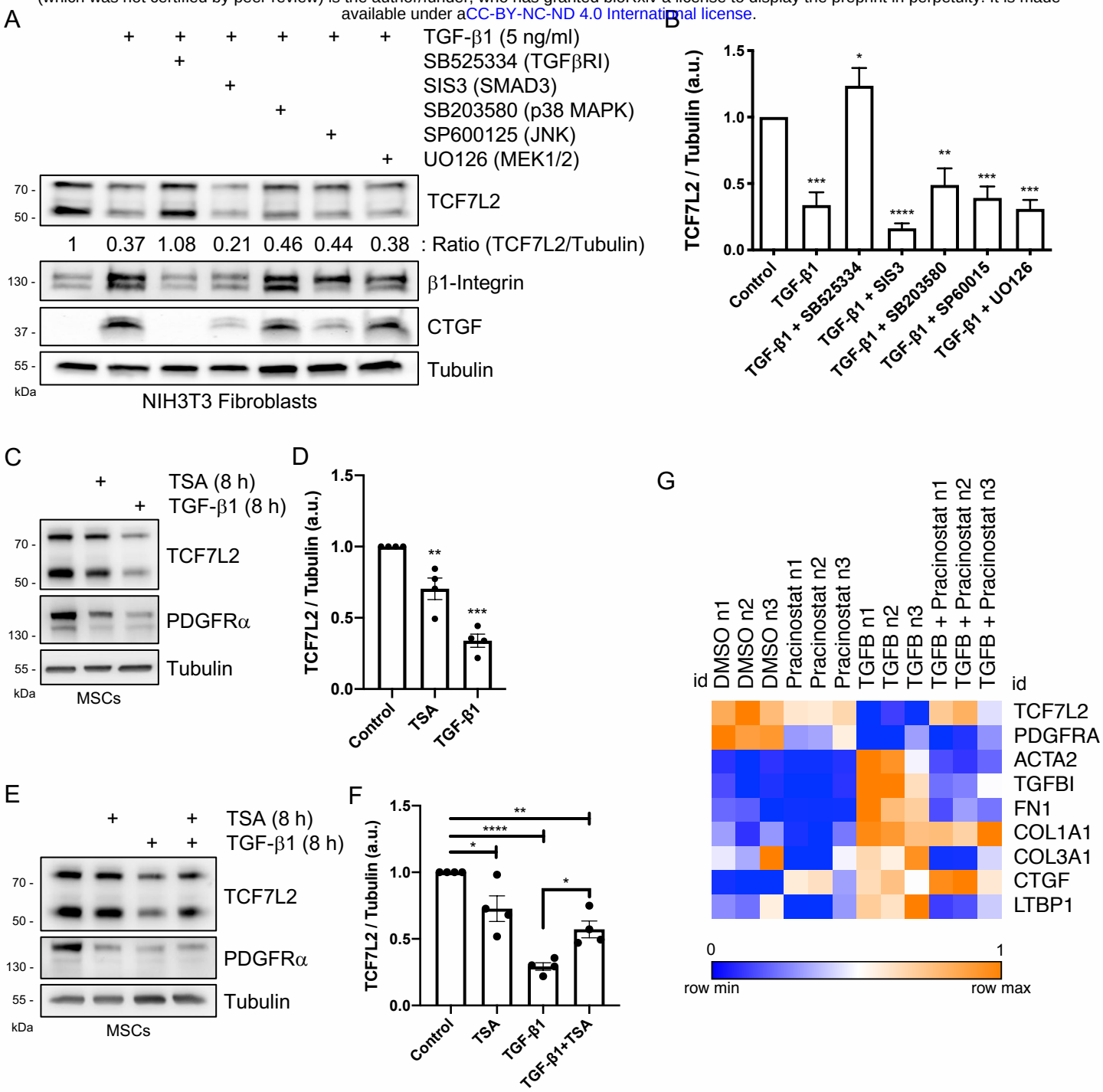

Fig. 5. Histone deacetylases participate in TGF-β-mediated repression of TCF7L2 expression.

(A) Representative western blot analysis showing TCF7L2, β1-Integrin, and CCN2/CTGF protein levels after TGF-β1 and SB525334, SIS3, SB203580, SP600125, and UO126 pharmacological co-treatments. Tubulin was used as the loading control. (B) Quantification of TCF7L2 protein expression. ****P<0.0001; ***P<0.001; **P<0.005; *P<0.05; by one-way ANOVA with Dunnett's post-test; n=5. (C) Representative western blot analysis showing TCF7L2 and PDGFRα protein levels after TGF-β1 (5 ng/ml) and Trichostatin A (TSA) (10 μM) treatments (8 h). Tubulin was used as the loading control. (D) Quantification of TCF7L2 protein expression. ***P<0.001; **P<0.005 by one-way ANOVA with Dunnett's post-test; n=3. (E) Representative western blot analysis showing TCF7L2 and PDGFRα protein levels after TGF-β1 (5 ng/ml) and Trichostatin A (TSA) (10 μM) co-treatments (8 h). Tubulin was used as the loading control. (F) Quantification of TCF7L2 protein expression. ****P<0.0001; **P<0.005; *P<0.05 by one-way ANOVA with Dunnett's post-test; n=3. (G) Heat map showing expression changes of *Tcf7l2* that are significantly repressed by TGFβ and reversed by pracinostat. Known pro-fibrotic mediators that are increased significantly by TGFβ and reversed by pracinostat are also shown. Each row is normalized to itself. Each column, per treatment condition, represents an individual IPF lung fibroblast donor (n=3).

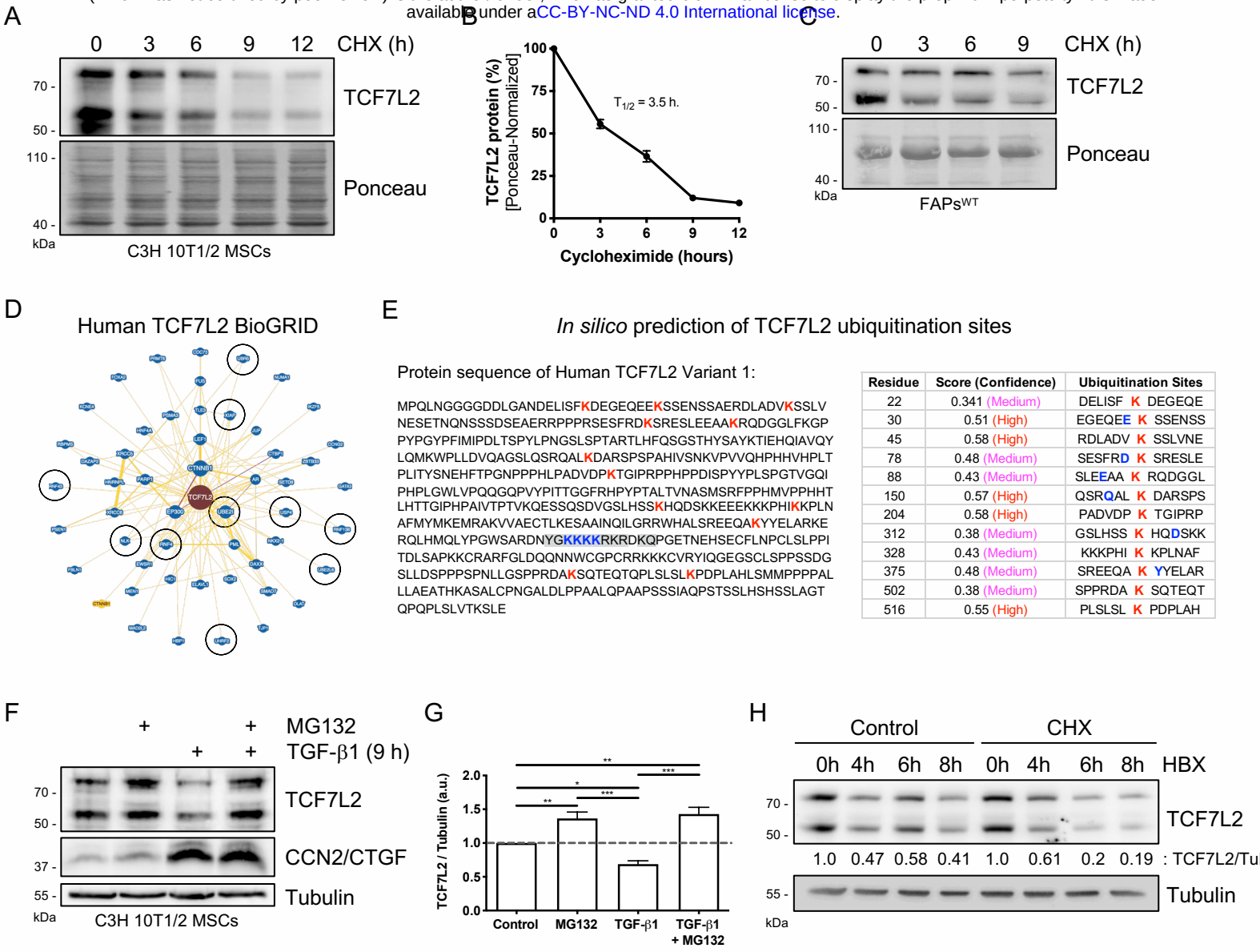

Fig. 6. TGF-β signaling impairs TCF7L2 protein stability via the ubiquitin proteasome system in mesenchymal stromal cells.

(A) Representative western blot analysis showing TCF7L2 protein levels after treatment with cycloheximide (CHX) (30 μg/ml) at different time points (0, 3, 6, 9, 12 h) in C3H/10T1/2 mesenchymal progenitor cells. Ponceau was used as the loading control. (B) Quantification of three independent experiments showing TCF7L2 protein levels (as a percentage [%]) after CHX treatment. (C) Representative western blot analysis showing TCF7L2 protein levels after treatment with cycloheximide (CHX) (30 μg/ml) at different time points (0, 3, 6, 9 h) in wild-type skeletal muscle FAPs. (D) (A) BioGRID interactome analysis of the human TCF7L2 protein. Black circles mark the protein-protein interaction between TCF7L2 and RNF4, RNF43, RNF138, NLK, UHRF2, UBE2I, UBE2L6, USP4, UBR5, and XIAP. (E) *In silico* prediction of TCF7L2 ubiquitination sites, showing the aminoacidic sequence of human TCF7L2 protein variant 1. Potential TCF7L2-ubiquitinated lysine residues were ranked and are shown in *blue*. http://www.ubpred.org; http://bdmpub.biocuckoo.org/. (F) Representative western blot analysis showing TCF7L2 and CCN2/CTGF protein levels in TGF-β1 (1 ng/ml) and MG132 (15 μM) treatments in C3H/10T1/2 MSCs for 9 h. Tubulin was used as the loading control. (G) Quantification of TCF7L2 protein levels. ***P<0.001; **P<0.005; *P<0.05 by one-way ANOVA with Dunnett's post-test; n=6. (H) Representative western blot analysis from three independent experiments that evaluate total levels of TCF7L2 following USP7 small-molecule inhibitor HBX 41108 (10μM) and CHX (30 μg/ml) treatments at different time points (0, 4, 6, 8 h) in C3H/10T1/2 MSCs. Tubulin was used as the loading control.

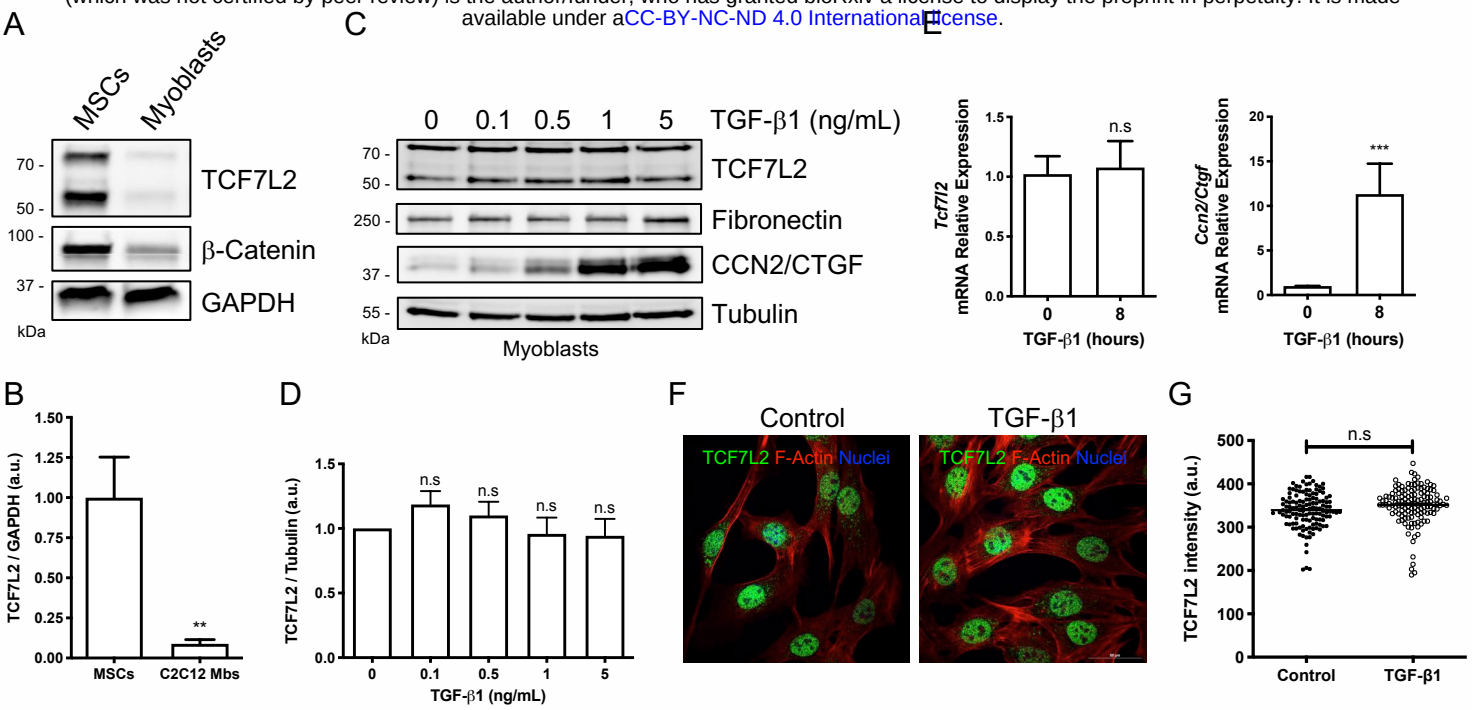

Fig. 7. The expression of TCF7L2 remains unchanged in response to TGF-β in myoblasts.

(A) Representative western blot analysis from three independent experiments, evaluating TCF7L2 and β-Catenin protein levels in proliferating C3H/10T1/2 MSCs and C2C12 myoblasts. GAPDH was used as the loading control. (B) Quantification of TCF7L2 protein levels. ***P*<0.005 by two-tailed Student's t-test. *n*=3. (C) Representative western blot analysis showing TCF7L2, fibronectin, and CCN2/CTGF protein levels after treatment with different concentrations of TGF-β1 for 24 h. (D) Quantification of TCF7L2 protein levels. n.s, not significant by two-tailed Student's t-test. *n*=3. (E) *Tcf7l2* and *CCN2/CTGF* mRNA expression levels were analyzed by quantitative PCR in C2C12 myoblasts after 8 h of treatment with TGF-β1 (5 ng/ml). ****P*<0.001; n.s, not significant by two-tailed Student's t-test. *n*=3. (F) Representative Z-stack confocal images showing localization of TCF7L2 (*green*) and F-actin (*red*) in control and TGF-β1-treated (24 h) C2C12 myoblasts. Scale bar: 50 μm. (G) Quantification of the TCF7L2 fluorescence intensity in C2C12 myoblasts. Each dot represents a single cell quantified were a ROI area was previously defined. n.s; not significant by two-tailed Student's t-test. *n*=3. (a.u.: arbitrary units).

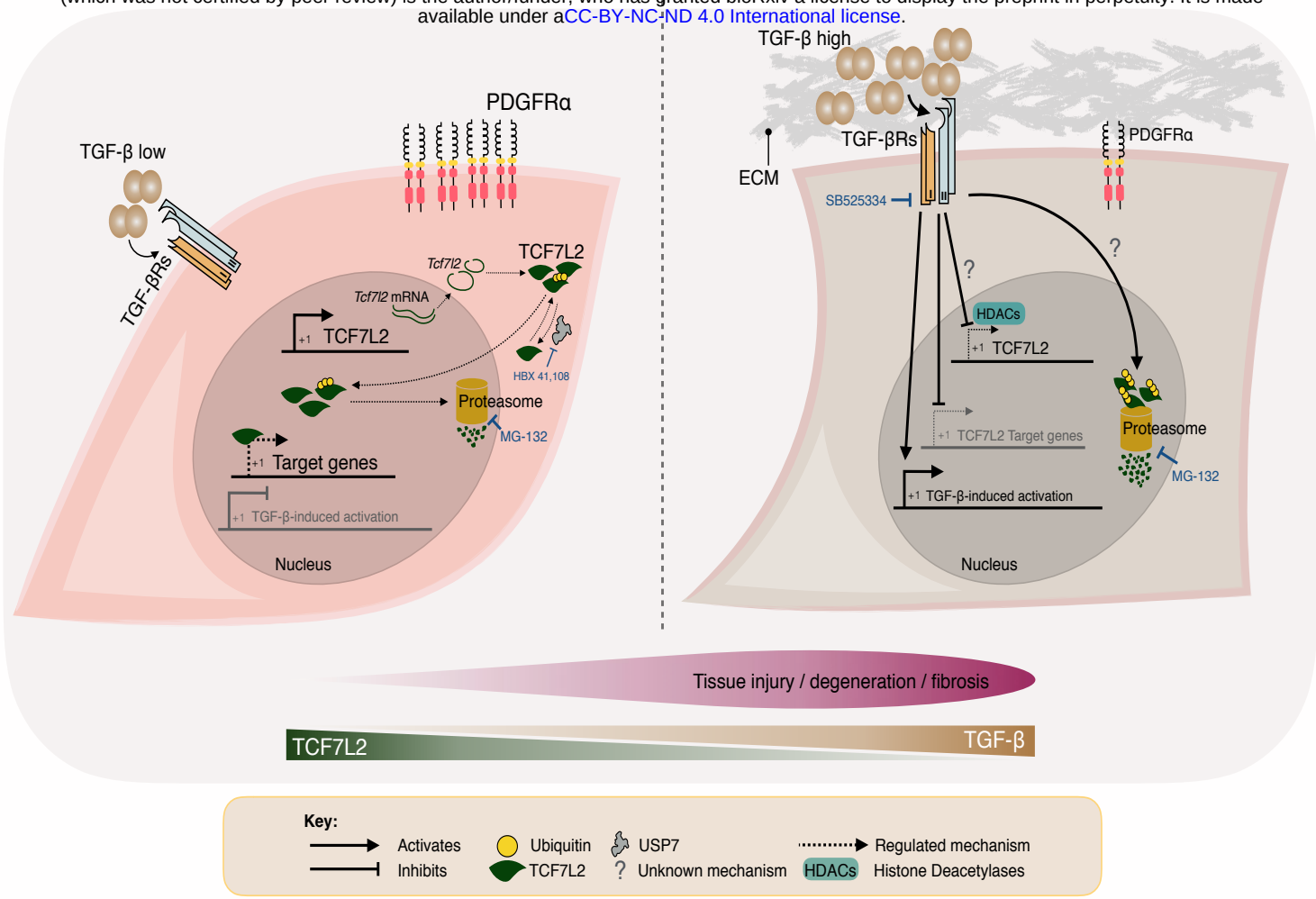

Fig. 8. Model of TGF-β regulation of fibroblast cell fate transition and the Wnt TCF7L2 gene expression regulatory network.

MSCs and fibroblasts express high levels of TCF7L2 in resting state, but low levels when differentiated and/or post-activation through extracellular TGF-β. *Tcf7l2* gene expression is active in unstimulated MSCs, and therefore, it continuously produces TCF7L2 protein. TCF7L2 transcription factor mainly localizes to the cell nucleus where recognized its target genes to activate or repress their gene expression depending on the cell context and transcriptional partners. The ubiquitin-proteasome system constantly regulates TCF7L2 proteostasis. Following tissue damage, TGF-β ligands released from macrophages (paracrine) and FAPs (autocrine) bind to TGF-β receptors (TGFBR1, TGFBR2 and TGFBR3) and activate TGFBR-dependent signaling cascades downregulating TCF7L2 expression and impairing TCF7L2-dependent gene expression. Mechanistically, inhibition of the 26S proteasome activity with MG132 blocks TGF-β-mediated TCF7L2 protein degradation. Also, HDACs inhibitors attenuated TGF-β-mediated TCF7L2 expression repression.